Palladium(II) β-Agostic Alkyl Cations and Alkyl Ethylene Complexes: Investigation of Polymer Chain Isomerization Mechanisms

Leigh H. Shultz, Daniel J. Tempel,† and Maurice Brookhart*

Contribution from the Department of Chemistry, University of North Carolina at Chapel Hill, CB 3290 Venable Hall, Chapel Hill, North Carolina 27599-3290

Received April 26, 2001

Abstract: A series of stable dialkyl complexes of Pd, (α-diimine)PdR_2 (α-diimine = aryl-substituted diimine, R = *n*-Pr, *n*-Bu, *i*-Bu), have been prepared via Grignard alkylation of the corresponding (α-diimine)$PdCl_2$ complexes. Protonation of these dialkyl species at low temperature results in loss of alkane and formation of cationic Pd β-agostic alkyl complexes, which have been observed as intermediates in the polymerization of ethylene and propylene by these Pd catalysts. Studies of the structure and dynamic behavior of these alkyl complexes are presented, along with the results of trapping reactions of these species with ligands such as NCMe, CO, and C_2H_4. Trapping with ethylene results in formation of cationic alkyl ethylene complexes which model the catalyst resting state in these systems. These complexes have been used to obtain mechanistic details and kinetic parameters of several processes, including isomerization of the alkyl ethylene complexes, associative and dissociative exchange with free ethylene, and migratory insertion rates of both primary and secondary alkyl ethylene species. These studies indicate that the overall branching observed in polyethylenes produced by these Pd catalysts is governed both by the kinetics of migratory insertion and by the equilibria involving the alkyl ethylene complexes.

Introduction

While several Ni(II)- and Co(III)-based complexes have been previously shown to function as ethylene polymerization catalysts,[1−8] the report[9] from these laboratories in 1995 of highly versatile Ni(II)− and Pd(II)−α-diimine-based catalysts of type **1** (Figure 1) has led to a resurgence of interest in development of late metal catalysts for olefin polymerizations and copolymerizations.[6−8,10−32]

Unique features of these diimine systems include (1) the ability to convert ethylene to high polymers with microstructures varying from nearly linear (semicrystalline) to hyperbranched (amorphous) with control over the degree of branching and

† Current address: Air Products and Chemicals, Inc., Allentown, PA 18195-1501.

(1) Keim, W.; Appel, R.; Storeck, A.; Kruger, C.; Goddard, R. *Angew. Chem., Int. Ed. Engl.* **1981**, *20*, 116−117.
(2) Möhring, V. M.; Fink, G. *Angew. Chem., Int. Ed. Engl.* **1985**, *24*, 1001−1003.
(3) Ostoja Starzewski, K. A.; Witte, J.; Reichert, K. H.; Vasiliou, G. In *Transition Metal Organometallic Catalysis Olefin Polymerization [Proceeding of the International Symposium]*; Kaminsky, W., Sinn, H., Eds.; Springer: Berlin, 1988; pp 349−360.
(4) Klabunde, U.; Ittel, S. D. *J. Mol. Catal.* **1987**, *41*, 123−134.
(5) Brookhart, M.; DeSimone, J. M.; Grant, B. E.; Tanner, M. J. *Macromolecules* **1995**, *28*, 5378−5380.
(6) Ittel, S. D.; Johnson, L. K.; Brookhart, M. *Chem. Rev.* **2000**, *100*, 1169−1203. This reference contains a comprehensive summary of the patent literature in this area.
(7) Britovsek, G. J. P.; Gibson, V. C.; Wass, D. F. *Angew. Chem., Int. Ed. Engl.* **1999**, *38*, 429−447.
(8) Hicks, F. A.; Brookhart, M. *Organometallics* **2001**, *20*, 3217−3219.
(9) Johnson, L. K.; Killian, C. M.; Brookhart, M. *J. Am. Chem. Soc.* **1995**, *117*, 6414−6415.
(10) Small, B. L.; Brookhart, M. *Macromolecules* **1999**, *32*, 2120−2130.
(11) Brookhart, M. S.; Johnson, L. K.; Killian, C. M.; Arthur, S. D.; Feldman, J.; McCord, E. F.; McLain, S. J.; Kreutzer, K. A.; Bennett, A. M. A.; Coughlin, E. B.; Ittel, S. D.; Parthasarathy, A.; Tempel, D. J. WO 9623010, 1996.
(12) Gates, D. P.; Svejda, S. A.; Onate, E.; Killian, C. M.; Johnson, L. K.; White, P. S.; Brookhart, M. *Macromolecules* **2000**, *33*, 2320−2334.
(13) Johnson, L. K.; Mecking, S.; Brookhart, M. *J. Am. Chem. Soc.* **1996**, *118*, 267−268.
(14) Killian, C. M.; Tempel, D. J.; Johnson, L. K.; Brookhart, M. *J. Am. Chem. Soc.* **1996**, *118*, 11664−11665.
(15) Killian, C. M.; Johnson, L. K.; Brookhart, M. *Organometallics* **1997**, *16*, 2005−2007.
(16) Mecking, S.; Johnson, L. K.; Wang, L.; Brookhart, M. *J. Am. Chem. Soc.* **1998**, *120*, 888−899.
(17) Small, B. L.; Brookhart, M.; Bennett, A. M. A. *J. Am. Chem. Soc.* **1998**, *120*, 4049−4050.
(18) Shultz, L. H.; Brookhart, M. *Organometallics*, in press.
(19) Svejda, S. A.; Johnson, L. K.; Brookhart, M. *J. Am. Chem. Soc.* **1999**, *121*, 10634−10635.
(20) Svejda, S. A.; Brookhart, M. *Organometallics* **1999**, *18*, 65−74.
(21) Tempel, D. J.; Brookhart, M. *Organometallics* **1998**, *17*, 2290−2296.
(22) Tempel, D. J.; Johnson, L. K.; Huff, R. L.; White, P. S.; Brookhart, M. *J. Am. Chem. Soc.* **2000**, *122*, 6686−6700.
(23) Cotts, P. M.; Guan, Z.; McCord, E.; McLain, S. *Macromolecules* **2000**, *33*, 6945−6952.
(24) Britovsek, G. J. P.; Gibson, V. C.; Kimberly, B. S.; Maddox, P. J.; McTravish, S. J.; Solan, G. A.; White, A. J. P.; Williams, D. J. *Chem. Commun.* **1998**, 849−850.
(25) Eilerts, N. W. WO 9915569, 1999.
(26) Guan, Z. B.; Cotts, P. M.; McCord, E. F.; McLain, S. J. *Science* **1999**, *283*, 2059−2062.
(27) Jurkiewicz, A.; Eilerts, N. W.; Hsieh, E. T. *Macromolecules* **1999**, *32*, 5471−5476.
(28) McCord, E. F.; McLain, S. J.; Nelson, L. T. J.; Arthur, S. D.; Coughlin, E. B.; Ittel, S. D.; Johnson, L. K.; Tempel, D.; Killian, C. M. *Macromolecules* **2001**, *34*, 362−371.
(29) McLain, S. J.; McCord, E. F.; Johnson, L. K.; Ittel, S. D.; Nelson, L. T. J.; Arthur, S. D.; Halfhill, M. J.; Teasley, M. F.; Tempel, D. J.; Killian, C.; Brookhart, M. *Polym. Prepr. (Am. Chem. Soc., Div. Polym. Chem.)* **1997**, *38* (1), 772−773.
(30) McLain, S. J.; Feldman, J.; McCord, E. F.; Gardner, K. H.; Teasley, M. F.; Coughlin, E. B.; Sweetman, K. J.; Johnson, L. K.; Brookhart, M. *Macromolecules* **1998**, *31*, 6705−6707.

10.1021/ja011055j CCC: $20.00
Published on Web 11/01/2001

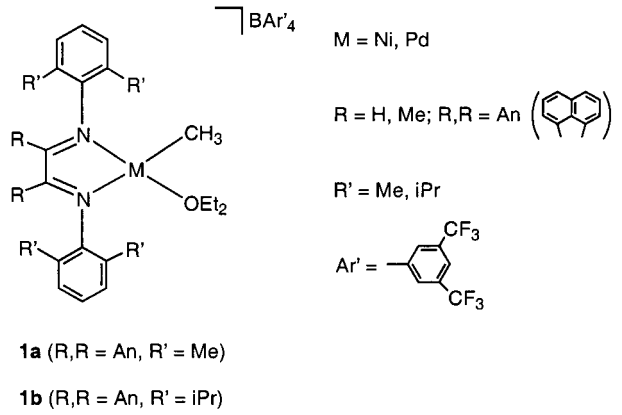

Figure 1. Ni(II)- and Pd(II)-based olefin polymerization catalysts.

Scheme 1. Proposed Mechanism for Propagation and Chain Walking

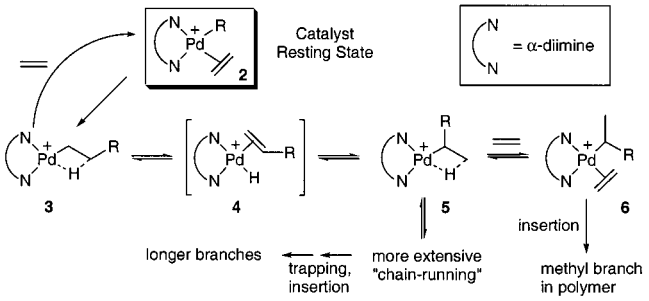

polymer architecture through ligand design and reaction variables,[9,12,23,26] (2) polymerization of α-olefins and internal olefins to polymers with unusual branching characteristics due to monomer insertion followed by migration of the metal to the terminal carbon of the chain prior to the next insertion,[9,28,33] (3) copolymerization of ethylene and α-olefins with alkyl acrylates to produce functionalized olefins with ester groups residing primarily on the ends of branches,[13,16] and (4) achievement of living polymerizations for both the Ni(II) and Pd(II) systems.[14,34]

While mechanistic investigations of both Ni(II)[19] and Pd(II)[9,18,22] diimine systems have been reported, the less reactive Pd(II) systems have thus far provided the most detailed information. The general mechanism for chain propagation of ethylene by a diimine palladium catalyst is shown in Scheme 1.

The following features have been clearly established through low-temperature NMR studies:

(1)The catalyst resting state is the alkyl ethylene complex. The turnover-limiting step is the migratory insertion of this species, where $\Delta G^{\ddagger}$ for insertion ranges from 17.5 to 18.8 kcal/mol and decreases with ligand bulk.

(2) Following insertion, the cationic palladium intermediate formed is a highly dynamic β-agostic alkyl complex.[21,35,36] Formation of branches results from "chain-walking" in this intermediate via a series of β-hydride elimination/readdition reactions,[2] as shown in Scheme 1.

Scheme 2. Equilibria in Propyl Agostic Species and Propyl Ethylene Complexes

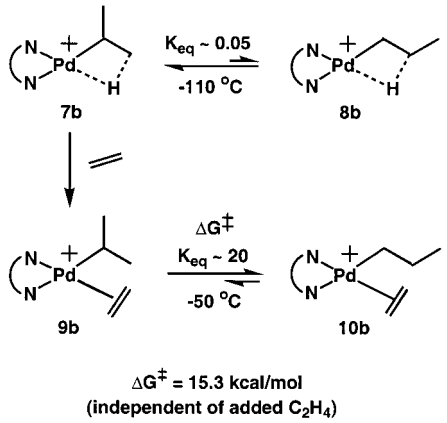

(3) Loss of ethylene from the "trapped" alkyl ethylene species is faster than migratory insertion of these species; i.e., **5** ⇄ **6** is a reversible reaction.

(4) Primary alkyl agostic species are less stable than the secondary agostic species, while the primary alkyl ethylene complexes are more stable than the secondary alkyl olefin complexes.[21] This latter trend was demonstrated with the simple palladium propyl complexes shown in Scheme 2.

The overall free energy diagram constructed for Scheme 2 is shown in Figure 2. We have established that the transition state for conversion of **9b** to **10b** involves trapping of **8b** and not conversion of the secondary agostic complex **7b** to the primary agostic species **8b** via β-elimination/readdition. Only an upper barrier limit of $\Delta G^{\ddagger} < 10.7$ kcal/mol for conversion of **7b** to **8b** (β-elimination) could be estimated. However, using a labeled agostic ethyl complex, **11b**, an accurate barrier for β-elimination of $\Delta G^{\ddagger} = 7.1$ kcal/mol (−55 °C) has been determined (Scheme 3).[18]

While the propyl complexes shown in Scheme 2 have provided significant insight into the mechanism of polymerization, the three-carbon chain is not a particularly good model for polymerization intermediates where agostic alkylpalladium complexes may bear alkyl substituents at both C_α and C_β. As a more realistic model, we report here the generation, structure, chemistry, and dynamics of (α-diimine)Pd butyl complexes and their corresponding ethylene complexes. These investigations illuminate many new mechanistic features of the polymerization reaction and provide a much more detailed description of the

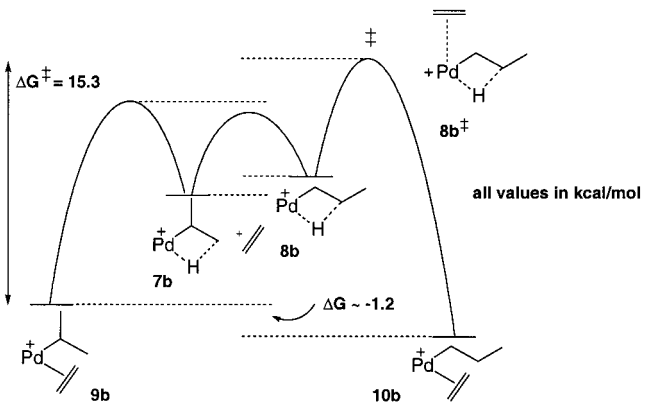

Figure 2. Free energy profile for the isomerization of propyl ethylene complex **9b**.

(31) Pappalardo, D.; Mazzeo, M.; Pellechia, C. *Macromol. Rapid Commun.* **1997**, *18* (12), 1017.
(32) Younkin, T. R.; Connor, E. F.; Henderson, J. I.; Friedrich, S. K.; Grubbs, R. H.; Bansleben, D. A. *Science* **2000**, *287*, 460−462.
(33) Leatherman, M. D.; Brookhart, M. *Macromolecules* **2001**, *34*, 2748−2750.
(34) Gottfried, A. C.; Brookhart, M. *Macromolecules* **2001**, *34*, 1140−1142.
(35) Brookhart, M.; Green, M. L. H. *J. Organomet. Chem.* **1983**, *250*, 395−408.
(36) Brookhart, M.; Green, M. L. H.; Wong, L.-L. *Prog. Inorg. Chem.* **1988**, *36*, 1−124.

Scheme 3. Isomerization of the Agostic Ethyl Cation **11b**

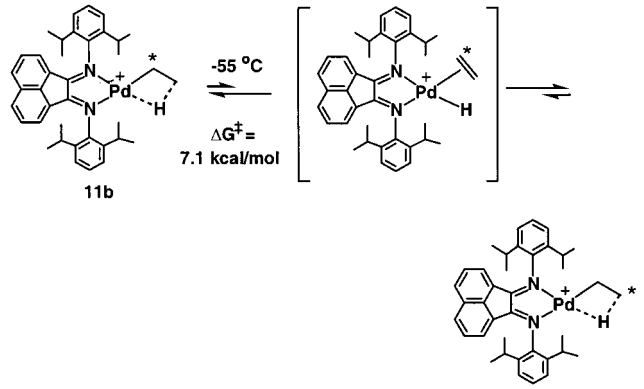

way in which branching is controlled by a combination of the kinetics for migratory insertion and the relative stabilities of primary and secondary alkyl olefin complexes. These findings are in good general agreement with the results of DFT calculations by Ziegler et al.[37,38]

Results

Synthesis of (α-Diimine)palladium(II) Dialkyl Species. Synthesis of the di-*n*-propyl (**13a,b**), di-*n*-butyl (**14a,b**), and diisobutyl (**15a,b**) complexes was accomplished by addition of 2 equiv of the corresponding Grignard reagent (*n*-PrMgCl, *n*-BuMgCl, or *i*-BuMgCl in Et_2O) to a cold slurry of the (α-diimine)$PdCl_2$ complex (**12a** or **12b**) in Et_2O (eq 1).

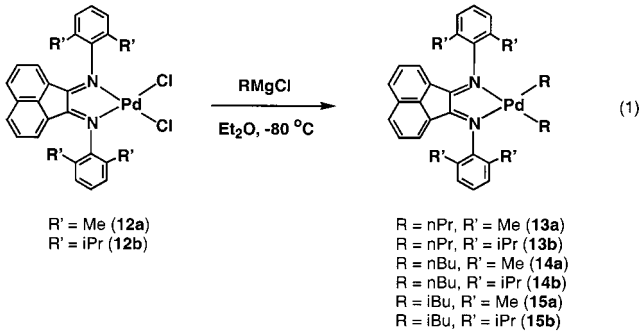

(1)

The dialkyl complexes were isolated as red-brown solids in moderate yields after filtration of the reaction mixture through a column of Florisil under argon. ^{1}H NMR spectra of **13a,b**−**15a,b** in CD_2Cl_2 at ambient temperature indicate that they possess two planes of symmetry, as expected: one containing the square plane of the metal center and one bisecting the two cis alkyl moieties. All of the species show one set of acenaphthyl *ortho* protons between 6 and 7 ppm, a sensitive indicator of symmetry. The two alkyl groups on the Pd center are equivalent, and the Pd center shields the α-CH_2 protons, often moving them upfield of the β-CH_2 (e.g. the β-CH_2 in **13a** resonates at 1.18 ppm, while the α-CH_2 signal appears at 0.89 ppm). The dialkyl complexes are surprisingly stable in solution but do decompose after days at room temperature to give alkanes, alkenes, and unidentified Pd(0) species due to β-H elimination followed by loss of olefin and reductive elimination; the di-*n*-butyl complexes **14a,b**, for example, decompose to give butane and internal butenes (Scheme 4).

Although 1-butenes should be the initial product of β-H elimination from a dibutyl species, they are not observed, and

Scheme 4. Thermal Decomposition of Palladium(II) Dibutyl Complex **14b**

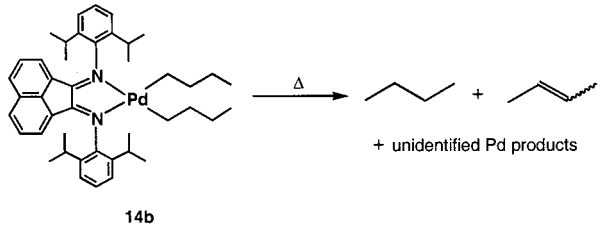

it is likely that they are rapidly isomerized by a Pd species to the more stable internal alkenes. These results are consistent with the products of decomposition seen from thermolysis of (2,2′-bipyridine)$PdEt_2$, an electronically similar d^8 system with accessible β-hydrogens.[39,40]

Generation of Agostic Alkyl Species. (α-Diimine)Pd(propyl)$^+$ Complexes. Treatment of the di-*n*-propyl complexes **13a,b** with $H(OEt_2)_2BAr'_4$ (Ar′ = 3,5-$(CF_3)_2C_6H_3$)[41] in $CDCl_2F$ at −80 °C results in formation of clear orange solutions; propane is evident in the ^{1}H NMR spectra. The products of these protonations were identified as the agostic isopropyl complexes **7a,b** by comparison of their spectral data with that published for the identical complexes made by insertion of ethylene into the Pd methyl cation (eq 2).[21,22]

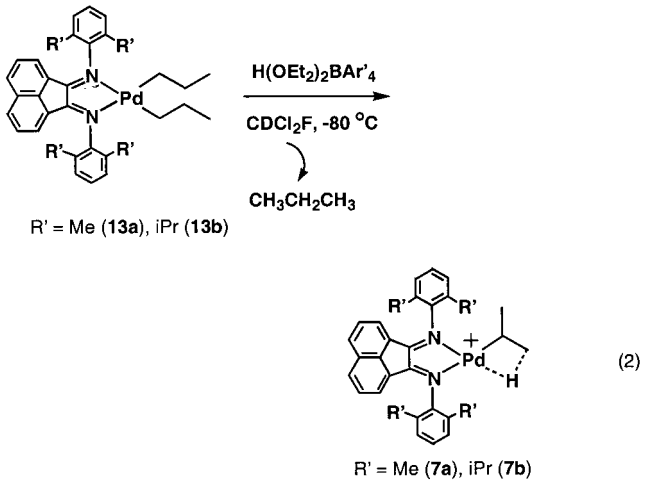

(2)

The triplet observed at −8.00 ppm at −120 °C in the ^{1}H NMR spectrum exhibits a $^2J_{HH}$ = 17 Hz (**7b**), diagnostic of an agostic alkyl species.[35,36] No doublet, corresponding to the *n*-propyl species, is observed, as was the case with the propyl complexes observed from insertion of ethylene into the Pd methyl cation. Complex **7a** shows similar behavior; the agostic hydrogen resonates as a triplet ($^2J_{HH}$ = 16 Hz) at −7.85 ppm at −120 °C.

Generation of (α-Diimine)Pd(butyl)$^+$ Complexes via Insertion. In the same way that a single insertion of ethylene into a Pd−methyl bond was used to generate Pd−propyl complexes,[21,22] low-temperature preparation of the methyl propylene complex **16b** followed by warming to −13 °C to induce insertion yields Pd−butyl complexes. As shown in Scheme 5, insertion can occur in a 1,2 or 2,1 manner, where complexes

(37) Michalak, A.; Ziegler, T. *Organometallics* **1999**, *18*, 3998−4004.
(38) Michalak, A.; Ziegler, T. *Organometallics* **2000**, *19*, 1850−1858.
(39) Sustmann, R.; Lau, J. *Chem. Ber.* **1986**, *119*, 2531−2541.
(40) Sustmann, R.; Lau, J.; Zipp, M. *Recl. Trav. Chim. Pays-Bas* **1986**, *105*, 356−359.
(41) Brookhart, M.; Grant, B.; Volpe Jr., A. F. *Organometallics* **1992**, *11*, 3920−3922.

Scheme 5. Formation of Agostic Butyl Complexes via Insertion of Propylene into a Pd−Methyl Bond

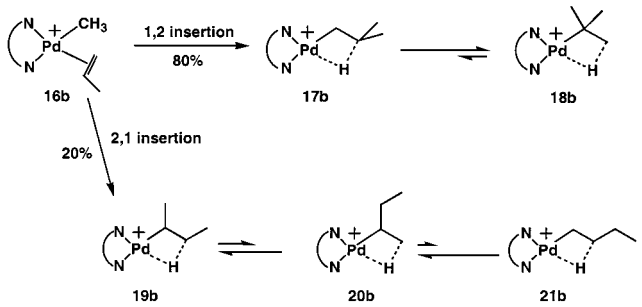

17b (1,2 insertion) or **19b** (2,1 insertion) are the initial products.

Although a complex mixture of isomers is formed, the Pd−*tert*-butyl complex, **18b** (formed from isomerization of the initial 1,2 insertion product, **17b**), clearly constitutes 80% of the mixture. In the static ^{1}H NMR spectrum (−110 °C in $CDCl_2F$), the agostic proton appears as a well-resolved triplet at −7.12 ppm ($^2J_{HH}$ = 15 Hz). Although the β-CH_2 is obscured, the two nonagostic methyl groups are equivalent and appear as a broad 6H singlet at 0.60 ppm. As the sample is warmed, the agostic H signal broadens due to the rotation of the agostic methyl group (C_α–C_β rotation), while the methyl signals at 0.60 ppm also broaden due to rotation about the Pd−C_α bond, which interchanges the agostic and nonagostic methyl groups. At 0 °C, the three methyl groups are now exchanging rapidly on the NMR time scale and appear as an averaged 9 H singlet at −0.20 ppm. The ligand peaks remain sharp (for example, two well-resolved ortho ^{1}H signals for **19b** appear at 6.33 and 6.63 ppm) and indicate that there is no rapid side-to-side isomerization of the *tert*-butyl alkyl group, consistent with the previously observed behavior of the Pd−isopropyl complex.[21] The structural assignments above have been verified by quantitative generation of **18b** by an independent route (see below).

The minor, complex series of resonances from 2,1 insertion are largely obscured by **18b** and are difficult to assign in these spectra. However, these isomers have been independently generated through the protonation of (α-diimine)Pd($(CH_2)_3CH_3)_2$ complexes, and a full description of their structure and dynamics is outlined below.

Generation of (α-Diimine)Pd(*tert*-butyl)$^+$ Complexes via Protonation of (α-Diimine)Pd($CH_2CH(CH_3)_2)_2$ Complexes. Protonation of the (α-diimine)Pd(diisobutyl) complexes (**15a,b**) at −80 °C in $CDCl_2F$ results in formation of the agostic *tert*-butyl complexes **18a,b** (eq 3).

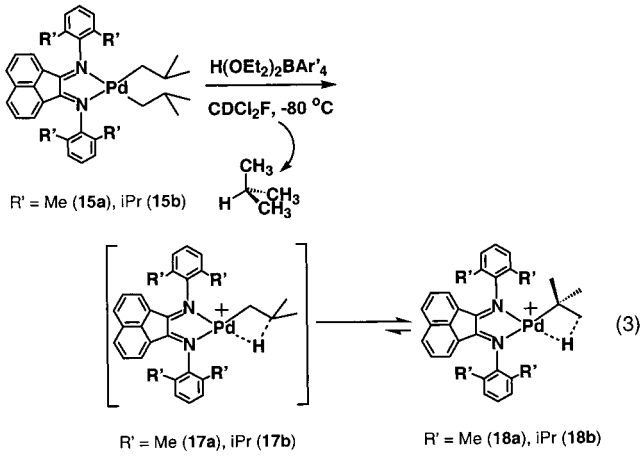

(3)

Scheme 6. Trapping of Agostic *tert*-Butyl Complexes **18a,b** with NCMe

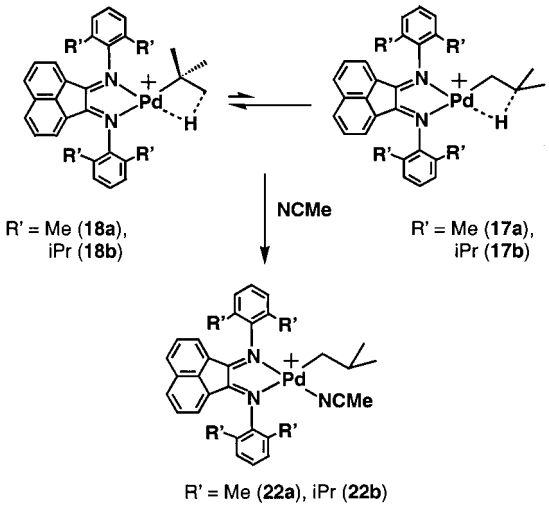

^{1}H NMR signals for **18b** generated by protonation are identical to those observed from insertion of propylene. At −110 °C, the agostic hydrogen of **18a** resonates as a triplet ($^2J_{HH}$ = 15 Hz) at −7.03 ppm, with the nonagostic methyl groups appearing at 0.56 ppm. The variable-temperature behavior of **18a** is similar to that previously described for **18b**. Overall, signals for **18a,b** are sharp and well-resolved at −110 °C, and no agostic isobutyl species (<5%) can be detected. These observations are consistent with the previous observation that the β-agostic Pd−isopropyl complex is strongly favored over the *n*-propyl complex.

Trapping Reactions of 18a,b. Trapping the agostic *tert*-butyl complexes (**18a,b**) with acetonitrile leads to formation of the isobutyl acetonitrile complexes, **22a,b** (Scheme 6).

No *tert*-butyl acetonitrile complex is observed, though, in trapping the agostic Pd−isopropyl complex, the isopropyl acetonitrile complex is not only the kinetic product but is also thermodynamically favored over the *n*-propyl acetonitrile complex.[22] It is unclear whether the isobutyl acetonitrile complex is formed by trapping of the small (unobservable) amount of agostic isobutyl complex in equilibrium with the agostic *tert*-butyl complex or if its formation results from initial trapping of the *tert*-butyl species and subsequent isomerization of the *tert*-butyl acetonitrile complex to the trapped isobutyl species via loss of acetonitrile, β-H elimination, reinsertion, and retrapping with acetonitrile.

In an attempt to trap the *tert*-butyl species, the smaller, more Lewis basic ligand CO was used; ^{13}CO was purged through a solution of the *tert*-butyl complex **18a** at −80 °C for 5 min. (^{13}CO was chosen for ease of product identification.) Use of CO does result in trapping of the agostic *tert*-butyl complex as the *tert*-butyl carbonyl complex **23a**, though a small (ca. 15%) amount of the isobutyl carbonyl species **24a** is initially present (Scheme 7).

At −90 °C in the ^{1}H NMR spectrum, the acenaphthyl *para* protons of **23a** are inequivalent, as expected, appearing as doublets at 8.08 and 8.06 ppm; likewise, the *ortho* hydrogens appear at 6.78 and 6.23 ppm. The two aryl rings on the diimine ligand are also inequivalent; the two sets of aryl methyl groups appear as singlets at 2.27 and 2.16 ppm. The *tert*-butyl group appears as a 9 H singlet at 0.99 ppm. The bound ^{13}CO resonates at 180.9 ppm in the ^{13}C NMR spectrum and is quite broad (ca. 60 Hz at half-height), possibly due to exchange with free ^{13}CO.

Scheme 7. Trapping the Agostic *tert*-Butyl Complex **18a** with CO

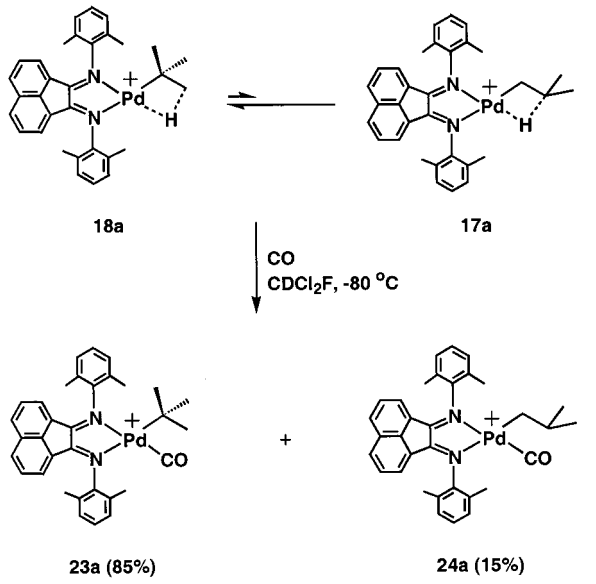

Warming the solution to −70 °C results in facile isomerization of the *tert*-butyl carbonyl complex (**23a**) to the isobutyl carbonyl complex **24a** (eq 4). Although the acenaphthyl *para*

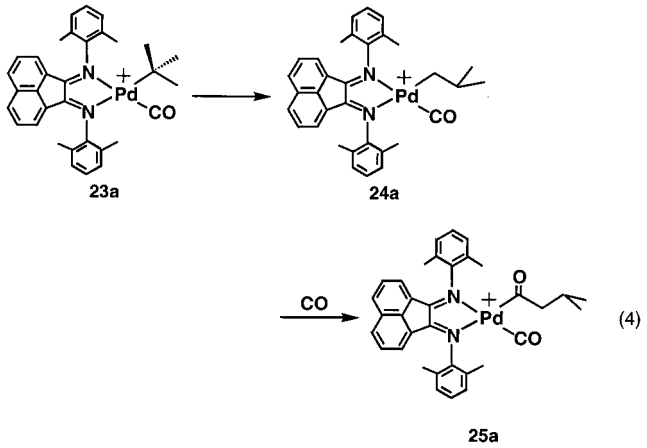

(4)

protons are partially obscured by those of the *tert*-butyl carbonyl complex **23a**, the *ortho* protons of **24a** are distinctly different, appearing at 6.83 and 6.49 ppm and growing with time. The methyl groups on the imine aryl rings at 2.31 and 2.19 are also distinct from those of the *tert*-butyl carbonyl complex. The Pd−isobutyl group exhibits a doublet at 2.01 ppm (methylene), a multiplet at 1.56 ppm (methine), and another doublet at 0.75 ppm (two methyls). Bound ^{13}CO appears as a sharp singlet at 175.0 ppm in the ^{13}C NMR spectrum. Quantitative formation of the isobutyl carbonyl complex **24a** from the *tert*-butyl carbonyl complex **23a** is not observed, since insertion of ^{13}CO into the Pd−isobutyl bond occurs competitively at this temperature (−70 °C), partially consuming the isobutyl carbonyl complex and forming a Pd−acyl carbonyl complex, **25a**. Only one set of acenaphthyl ligand peaks appear (two doublets at 8.12 and 8.09 ppm for the *para* protons and two doublets at 6.82 and 6.57 ppm for the *ortho* protons), indicating one major product. This species has a resonance in the ^{13}C NMR spectrum at 210.7 ppm, consistent with formation of an acyl species via insertion of ^{13}CO.[42] A broad peak is observed at 172.2 ppm, consistent with bound ^{13}CO exchanging with free ^{13}CO in

Scheme 8. Formation and Interconversion of Pd(butyl)$^+$ Complexes via Protonation

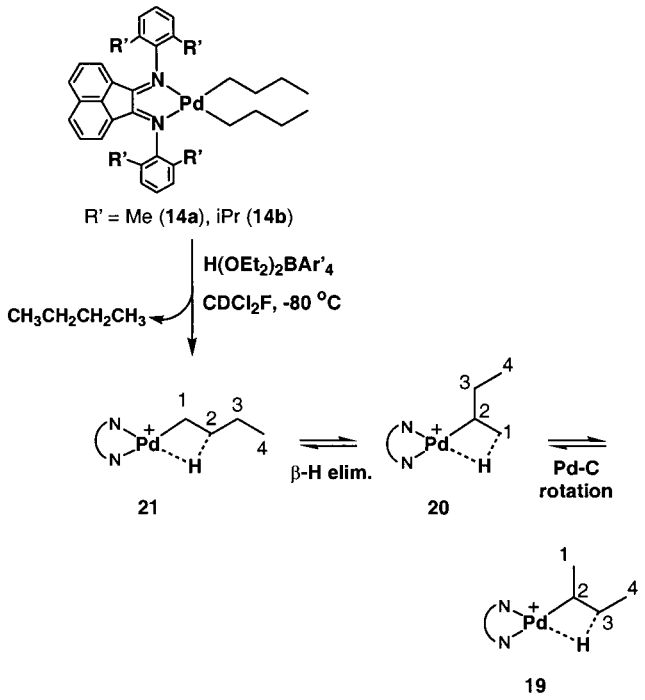

solution. A new isobutyl group appears in the alkyl region; a sharp doublet at 0.56 ppm is indicative of equivalent isobutyl methyl groups, while the methylene group appears as a triplet at 2.64 ppm from coupling to both the methine ^{1}H and ^{13}C-labeled acyl carbon ($^2J_{CH}$ = 6 Hz). **25a** decomposes upon further warming, with Pd(0) formation evident.

Formation of (α-Diimine)Pd(butyl)$^+$ Complexes from Protonation of (α-Diimine)Pd((CH$_2$)$_3$CH$_3$)$_2$ Complexes. Protonation of the di-*n*-butyl species **14a,b** produces only linear isomers and thus facilitates the identification of the products of 2,1-insertion of propylene into a Pd−methyl bond (see Scheme 5). The possible products, **21**, **20**, and **19**, are shown in Scheme 8 together with their modes of interconversion.

Loss of *n*-butane via protonolysis will initially form the agostic *n*-butyl complex **21**. β-H elimination and reinsertion will produce the agostic *sec*-butyl complex **20**, possessing an ethyl substituent at C$_\alpha$. The second *sec*-butyl isomer, **19**, is produced by simple release of the agostic interaction, rotation about the Pd−C$_\alpha$ bond, and agostic bond formation at C3. Species **21** is expected to be a negligible component of the mixture on the basis of the much greater stability of the agostic Pd−isopropyl complex relative to the Pd−*n*-propyl complex.[22]

Treatment of **14b** with H(OEt$_2$)$_2$BAr′$_4$ (CDCl$_2$F, −110 °C) results in formation of a mixture of β-agostic butyl isomers whose ^{1}H NMR spectrum in the high-field region is shown in Figure 3.

Kinetic trapping of these species by ethylene yields only (α-diimine)Pd(CH(CH$_3$)(CH$_2$CH$_3$))(CH$_2$=CH$_2$)$^+$ complexes, confirming that **21b** is not present in appreciable amounts in this mixture. The broad triplet at −8.01 ppm, which sharpens and appears only below −100 °C and shows a typical $^2J_{HH}$ = 16 Hz, can be assigned to the agostic *sec*-butyl species **20b**, leaving the two signals between −8.3 and −8.1 ppm which sharpen below −80 °C as attributable to **19b**.

(42) Rix, F. C.; Brookhart, M. *J. Am. Chem. Soc.* **1995**, *117*, 1137−1138.

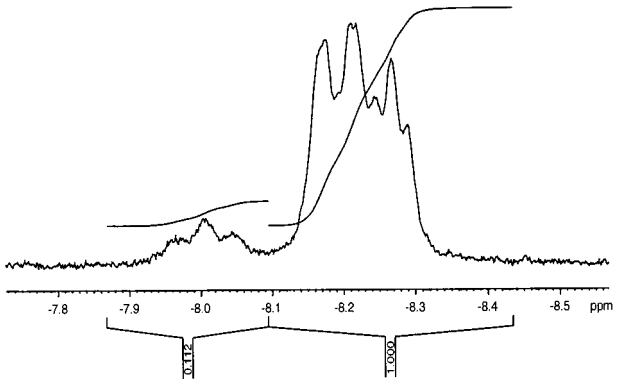

Figure 3. High-field region of the ^{1}H NMR spectrum ($CDCl_2F$, −110 °C) resulting from protonation of **14b**.

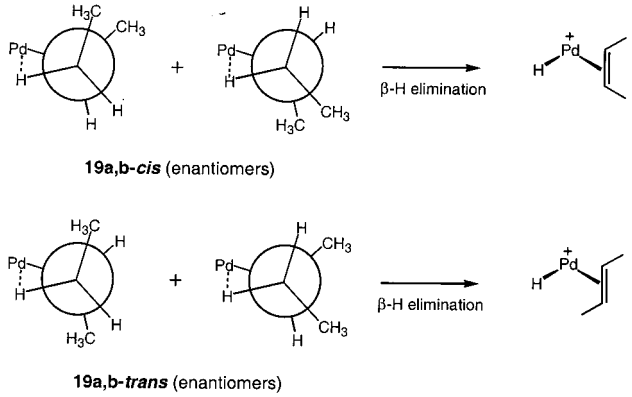

Figure 4. Cis and trans isomers of **19a,b**.

Scheme 9. Dynamic Processes in **19b**-*cis* That Equilibrate H_b and H_c

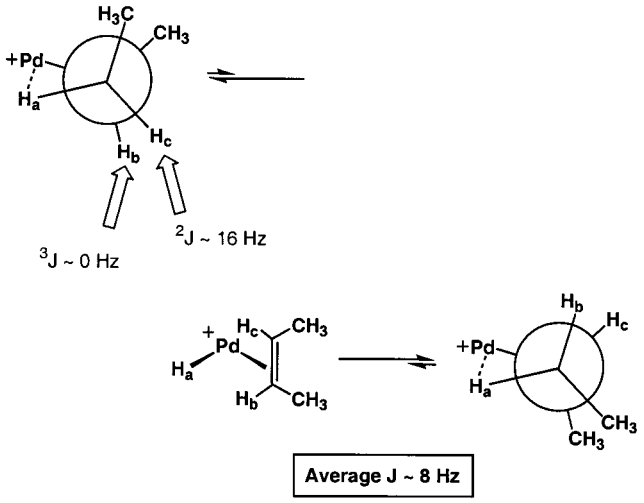

Since there is a significant barrier to rotation about the C_α–C_β bond[18,21] and because C_α and C_β each possess a methyl substituent, cis and trans rotational isomers are expected to be observable, as shown in Figure 4 (each isomer exists as a pair of enantiomers). The cis isomer yields a *cis*-2-butene hydride complex upon β-elimination, while the trans isomer yields a *trans*-2-butene hydride complex, as shown in Figure 4.

We assign the doublet at −8.19 ppm, with a typical geminal $^2J_{HH}$ = 16 Hz, to the static trans isomer, **19b**-*trans*. The unusual triplet at −8.27 ppm with a geminal $^2J_{HH}$ of only ca. 7 Hz is assigned to the *fluxional* cis isomer, **19b**-*cis*. The agostic proton from the cis rotamer appears as a triplet due to rapid β-H elimination and reinsertion (Scheme 9). This process interchanges H_b and H_c and results in the appearance of H_a as a triplet with an averaged J value of $J = (J_{ac} + J_{ab})/2$ = ca. (16 Hz + 0 Hz)/2 = ca. 8 Hz.

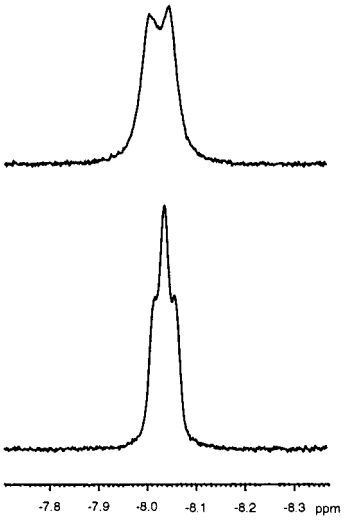

Figure 5. Variable-temperature ^{1}H NMR spectra of cyclopentyl agostic cation **27a** at −110 °C (top) and −80 °C (bottom).

Integration of the triplet at −8.01 ppm (**20b**) versus the two resonances upfield due to **19b**-*trans* and **19b**-*cis* yields the equilibrium constant for the species, K_{eq} = 8.9, corresponding to a free energy difference of −0.7 kcal/mol (eq 5).

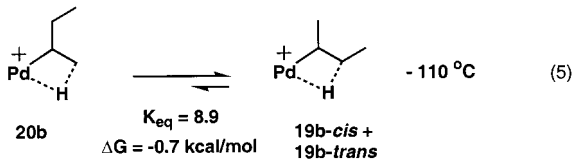

(5)

In an attempt to synthesize an agostic complex restricted to a cis conformation to compare to **19b**-*cis*, we were able to prepare and protonate a crude dicyclopentyl species **26a** (eq 6) to produce an agostic cyclopentyl complex, **27a**.

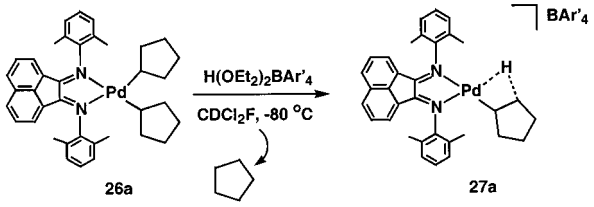

(6)

Despite several attempts, we were unable to obtain a completely pure sample of either the dicyclopentyl complex **26a** or the cyclopentyl agostic species **27a**; however, variable-temperature ^{1}H NMR analysis of the impure cyclopentyl complex **27a** provides strong support for the proposed structure of **19b**-*cis*, so we present these data. At −110 °C in $CDCl_2F$, the cyclopentyl agostic proton appears as a doublet at −8.04 ppm, $^2J_{HH}$ = 16 Hz.[30] Upon warming of the sample to −80 °C, however, the resonance collapses to a triplet, with a coupling constant $^2J_{HH}$ ~ 8 Hz (Figure 5).

The cyclopentyl complex is constrained in a cis configuration, making it quite similar to the cis *sec*-butyl rotamer **20b**-*cis* (Figure 6).

Thus, the similarity of the spectroscopic behavior of the *sec*-butyl rotamer **19b**-*cis* and the cyclopentyl agostic cation **27a**, which must be a cis species, support the structural assignment of **19b**-*cis*.

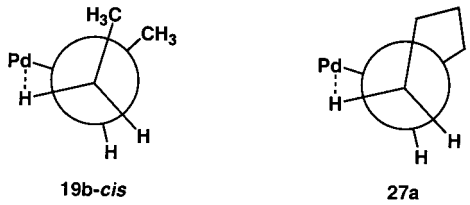

Figure 6. Structures of the cis *sec*-butyl rotamer **19b**-*cis* vs the cyclopentyl agostic cation **27a**.

Scheme 10. Formation of Ethyl Ethylene Complexes **30a,b**[BAr′$_4$]

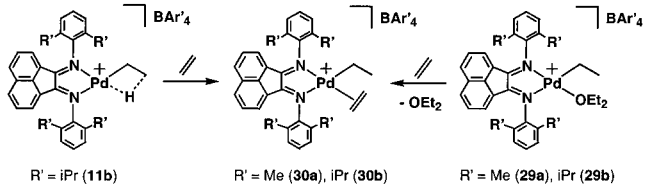

Protonation of the di-*n*-butyl complex **14a** gives similar results; the cis and trans rotational isomers are again observed, but none of the *sec*-butyl isomer **20a**, having an ethyl group on C_α, is present in the product mixture. The butyl complexes which are the products of protonation of **14a,b** (**28a,b**) can be obtained on a preparatory scale and give satisfactory elemental analyses. The static and dynamic ^{1}H NMR spectra of these cationic complexes are identical to those observed from in situ protonation. These isolated agostic butyl complexes can be used to generate butyl ethylene species as discussed below and will polymerize ethylene in an fashion identical with that of the Pd methyl ethylene complexes ((α-diimine)Pd(CH$_3$)(CH$_2$=CH$_2$)$^+$) previously published.[9,22]

Generation and Chemistry of (α-Diimine)palladium(II) Alkyl Ethylene Complexes. (α-Diimine)Pd(CH$_2$CH$_3$)(CH$_2$=CH$_2$)$^+$ Complexes. Addition of 1 or more equiv of ethylene to either the ethyl agostic cation [((2,6-(*i*-Pr)$_2$C$_6$H$_3$)N=C(An)C(An)=N(2,6-(*i*-Pr)$_2$C$_6$H$_3$))Pd(CH$_2$CH$_2$-μ-H)]BAr′$_4$ (**11b**) or to the ethyl ether complexes, [((2,6-(CH$_3$)$_2$C$_6$H$_3$)N=C(An)C(An)=N(2,6-(CH$_3$)$_2$C$_6$H$_3$))Pd(CH$_2$CH$_3$)(OEt$_2$)]BAr′$_4$ (**29a**) and [((2,6-(*i*-Pr)$_2$C$_6$H$_3$)N=C(An)C(An)=N(2,6-(*i*-Pr)$_2$C$_6$H$_3$))Pd(CH$_2$CH$_3$)(OEt$_2$)]BAr′$_4$ (**29b**), results in trapping of **11b** or displacement of the diethyl ether ligand, respectively, and quantitative formation of the ethyl ethylene cations **30a,b**[BAr′$_4$] (Scheme 10).[18]

Alternatively, the neutral diethyl complexes **31a,b** can be treated with B(C$_6$F$_5$)$_3$, a powerful Lewis acid known to abstract methide from transition metal methyl complexes.[43] Like Ph$_3$C$^+$,[44] B(C$_6$F$_5$)$_3$ abstracts hydride from C_β of the diethyl species **31a,b**, resulting in formation of the ethyl ethylene cations **30a,b**[HB(C$_6$F$_5$)$_3$] (eq 7).[45]

The ^{1}H NMR spectra of **30a,b**[BAr′$_4$] and **30a,b**[HB(C$_6$F$_5$)$_3$] are nearly identical (with the exception of the counterion resonances), differing only slightly in chemical shift. For brevity, only the spectra of **30a,b**[BAr′$_4$] will be discussed here; the reader is referred to the Experimental Section for the spectral data of **30a,b**[HB(C$_6$F$_5$)$_3$].[46] The ligand resonances for **30a**[BAr′$_4$]

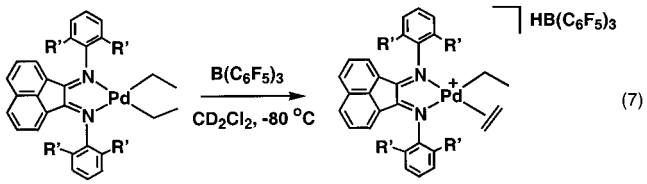

in CD_2Cl_2 at −80 °C show two inequivalent sides of the square planar complex as expected; for example, two sets of methyl groups (from the imine aryl rings) appear at 2.26 and 2.21 ppm. Bound ethylene (rotating rapidly on the NMR time scale) appears as a broad singlet at 4.60 ppm, upfield of free ethylene (5.4 ppm), while the Pd−ethyl group exhibits a quartet at 1.34 ppm (methylene) and a triplet at 0.43 (methyl). The data for **30b**[BAr′$_4$] are similar, indicating fast rotation of the bound ethylene and a plane of symmetry containing the square plane of the metal center.

Mechanism of Alkyl Ethylene Isomerization. When the Pd isopropyl ethylene complex **9b** is warmed, isomerization to the *n*-propyl ethylene complex **10b** occurs with a rate independent of [ethylene] at moderate ethylene concentrations. Though we believed this to be a process involving dissociation of ethylene, the lack of rate suppression by ethylene led us to investigate this general mechanism of isomerization further. In the case of the ethyl ethylene complexes, the isomerization is a degenerate one. Two mechanisms are possible, which are illustrated for a ^{13}C-labeled complex in Scheme 11.

Scheme 11. Possible Mechanisms for Alkyl Ethylene Isomerization

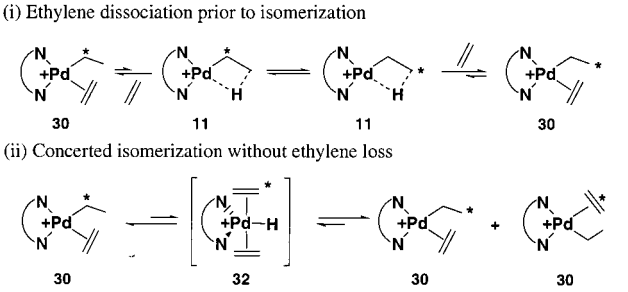

The first involves dissociation of ethylene to form the agostic ethyl complex **11**, which rapidly isomerizes before it is retrapped by ethylene. The second involves β-H elimination from the 16-electron ethylene complex, **30**, to produce a 5-coordinate, trigonal bipyramidal bis-olefin hydride species, **32**. Such a species could be the transition state; this process has been proposed by Ziegler, on the basis of DFT calculations, to account for chain transfer in the polymerization reactions of the Ni analogues.[47] Reinsertion of the olefin with opposite regiochemistry into the Pd−H bond would result in formation of the isomerized ethyl ethylene cation. Clearly, insertion of the other ethylene unit may also occur. We reasoned that if the actual mechanism involved a 5-coordinate species (Scheme 11ii), we should be able to isotopically label either the alkyl group or the bound ethylene moiety, and some of the label should eventually appear in the other moiety. Treatment of the singly ^{13}C-labeled agostic ethyl species **11b**-^{13}C (generated from

(43) Chen, E. Y.; Marks, T. J. *Chem. Rev.* **2000**, *100*, 1391−1434 and extensive references therein.

(44) For examples of β-H abstraction from transition metal alkyl complexes with trityl cation, see: (a) Cousins, M.; Green, M. L. H. *J. Chem. Soc.* **1963**, 889−894 (b) Mandon, D.; Toupet, L.; Astruc, D. *J. Am. Chem. Soc.* **1986**, *108*, 1320−1322 and ref 10.

(45) To our knowledge, this is the first example of β-H abstraction in a transition metal alkyl using B(C$_6$F$_5$)$_3$. We have also observed this process in similar Pd alkyl species such as (bpy)PdEt$_2$.

(46) The $^-$HB(C$_6$F$_5$)$_3$ anion is a good hydride donor above ca. −40 °C, resulting in decomposition of the Pd complexes above this temperature.

(47) Deng, L.; Margl, P.; Ziegler, T. *J. Am. Chem. Soc.* **1997**, *119*, 1094−1100.

Table 1. Rate Constants for Isomerization of **30b**-$^{13}C_\alpha[HB(C_6F_5)_3]$ in the Presence of Varying Equivalents of Ethylene at −55 °C

[Pd complex], M	$[C_2H_4]$, M	k (s^{-1})
0.014	0	3.64×10^{-5}
0.015	0.297	1.67×10^{-5}
0.014	0.440	1.44×10^{-5}

protonation of **31b**-$^{13}C_\alpha$) with unlabeled ethylene in CD_2Cl_2 at −80 °C affords the ethyl ethylene cation **30b**-$^{13}C[BAr'_4]$, having a ^{13}C label only on the ethyl moiety. Upon warming of this species to −55 °C and acquisition of successive $^{13}C\{^1H\}$ NMR spectra over hours, no ^{13}C label is observed in the bound ethylene; this observation supports the proposal that isomerization occurs via dissociation of ethylene (eq 8).[22]

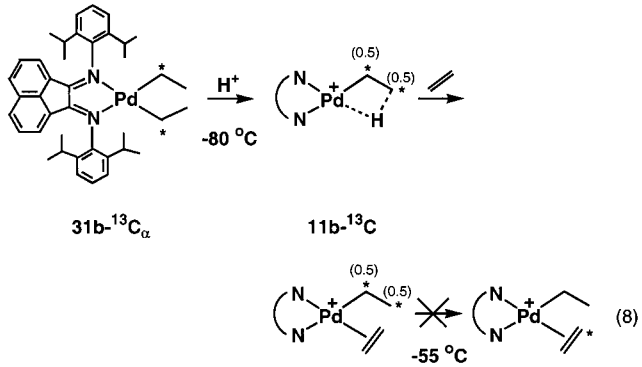

31b-$^{13}C_\alpha$ **11b**-^{13}C (8)

30b-$^{13}C[BAr'_4]$
(50% $^{13}C_\alpha$, 50% $^{13}C_\beta$)

The same ^{13}C-labeled diethyl complex (**31b**-$^{13}C_\alpha$) used to produce the labeled agostic ethyl complex **11b**-^{13}C above can be treated with $B(C_6F_5)_3$ to afford an ethyl ethylene complex, **30b**-$^{13}C_\alpha[HB(C_6F_5)_3]$, having one ^{13}C label at the α-carbon of the ethyl moiety and another ^{13}C label in the bound ethylene (eq 9).

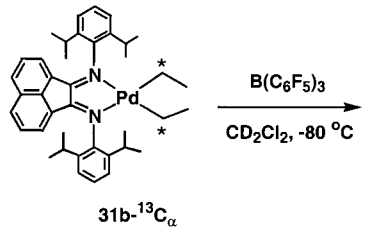

31b-$^{13}C_\alpha$

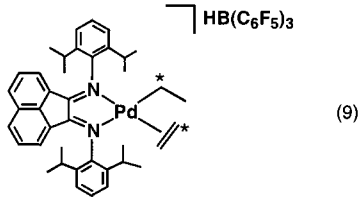

(9)

30b-$^{13}C_\alpha[HB(C_6F_5)_3]$

Use of $B(C_6F_5)_3$ to abstract hydride allows direct formation of the ethyl ethylene complex before significant isomerization can occur. Equilibration of the ^{13}C label between C_α and C_β can then be followed by ^1H NMR spectroscopy (eq 10).

Analysis of the kinetics yields $k_1 = k_{-1} = 3.6(0.1) \times 10^{-5}$ s^{-1} (−55 °C) and a barrier to dissociation of ethylene from the ethyl ethylene cation of $\Delta G^\ddagger = 17.1 \pm 0.1$ kcal/mol. Addition of large excesses of ethylene does slightly slow the rate of isomerization in this case (Table 1).

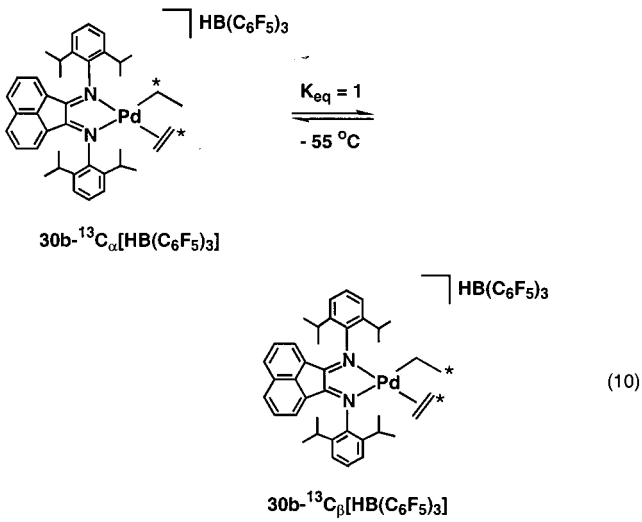

30b-$^{13}C_\alpha[HB(C_6F_5)_3]$

30b-$^{13}C_\beta[HB(C_6F_5)_3]$ (10)

Associative Exchange Rates. With evidence in hand that ethylene dissociates from the metal center during alkyl olefin isomerization, we wished to reexamine the mechanism of ethylene exchange with these ethyl ethylene cations. We have previously used the corresponding methyl ethylene complexes to obtain associative exchange rate constants in the presence of excess ethylene; steric bulk on the ligand aryl rings slows associative exchange.[22] In the case of a higher alkyl, however, exchange of bound ethylene with free ethylene in solution could possibly occur rapidly in a dissociative fashion (Scheme 12),

Scheme 12. Associative vs Dissociative Exchange with Free Ethylene

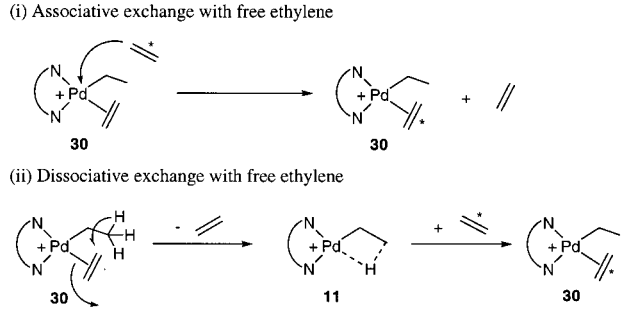

as formation of the β-C−H agostic interaction may aid in displacement of ethylene from the Pd center. This agostic participation is not possible in the methyl ethylene complexes, which do not have β-C−H bonds available.

The line width in the absence of ethylene exchange was measured in CD_2Cl_2 for the bound ethylene in **30a,b**[HB-$(C_6F_5)_3$]. Generation of these complexes in situ allowed easy access to the ethyl ethylene complexes with no excess ethylene in solution, since only 1 equiv of ethylene is generated per metal center by hydride abstraction. Line widths at half-height (ω) were then measured (in Hz) for the bound ethylene resonance in the presence of added ethylene at −85 °C, and rate constants for exchange were determined from the equation for the slow-exchange approximation, $k = \pi(\Delta\omega)/[C_2H_4]$, where $[C_2H_4]$ is the concentration of free ethylene in solution (determined by integration against the ligand resonances) (Table 2). The bound ethylene resonance is only distinct with less than ca. 5 equiv of ethylene in solution, after which it merges with the free ethylene resonance. The rate of ethylene exchange clearly increases as the concentration of ethylene in solution increases, consistent with associative exchange. Rate constants for exchange in the

Table 2. Second-Order Rate Constants for Ethylene Exchange at −85 °C

complex	rate const (M^{-1} s^{-1})	complex	rate const (M^{-1} s^{-1})
31a (Et)	5570	**31b** (Et)	950
33a (Me)	2600	**33b** (Me)	560

corresponding methyl ethylene complexes **33a,b** are shown for comparison.[22]

Ethyl Ethylene Migratory Insertion Rates. The ethyl ethylene complexes **30a,b** are unique in this system in that they are degenerate species; isomerization of the complex does occur but produces an identical ethyl ethylene complex. We had previously been unable to measure rates for migratory insertion of ethylene into different types of Pd−C bonds due to rapid equilibration of numerous alkyl isomers prior to insertion. Using turnover frequencies, only subsequent insertion barriers were obtained, which are average barriers for insertion into all types of Pd−C bonds in the system.[22] Using the ethyl ethylene complexes, however, barriers for migratory insertion of ethylene into only Pd−primary carbon bonds can be measured (eq 11).

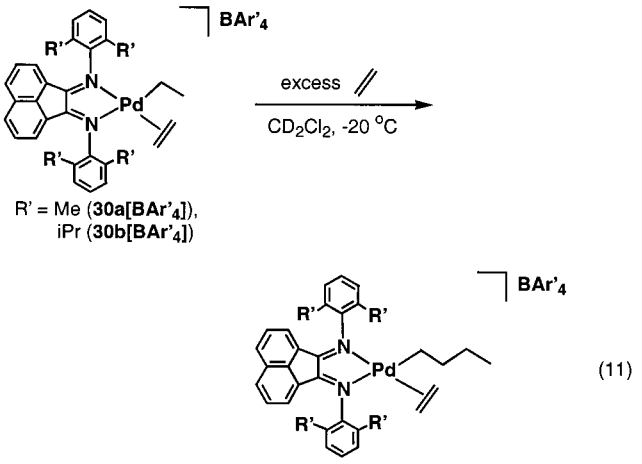

(11)

In the presence of 20 equiv of ethylene, loss of the ethyl resonances in the ^{1}H NMR spectra of **30a,b**[BAr′$_4$] was measured with respect to time, yielding $k = 3.31(0.05) \times 10^{-4}$ s^{-1} at −19 °C for **30a**, corresponding to $\Delta G^{\ddagger} = 18.9 \pm 0.1$ kcal/mol, and $k = 2.77(0.06) \times 10^{-4}$ s^{-1} at −24 °C for **30b**, corresponding to $\Delta G^{\ddagger} = 18.5 \pm 0.1$ kcal/mol.

(α-Diimine)Pd(CH$_2$CH(CH$_3$)$_2$)(CH$_2$═CH$_2$)$^+$ Complexes. When CD_2Cl_2 solutions of the agostic *tert*-butyl complexes **18a,b** were treated with 1 or more equiv or more of ethylene at −80 °C, no *tert*-butyl ethylene complexes (**34a,b**) were observed by ^{1}H NMR spectroscopy. Instead, only the isomerization products, the isobutyl ethylene complexes **35a,b**, are observed. This is consistent with the results seen when acetonitrile, a smaller ligand, is used to trap these species. The ligand resonances for complex **35b** indicate the expected asymmetry at the metal center; two doublets appear for both the acenaphthyl *para* protons (8.06 and 8.02 ppm) and the *ortho* protons (6.52 and 6.44 ppm). Bound ethylene resonates at 4.58 ppm as a singlet, indicating rapid rotation at this temperature. The isobutyl methylene hydrogens appear as a doublet ($J = 5.6$ Hz) at 1.38 ppm, the methine hydrogen appears as a multiplet at 0.95 ppm, and the two equivalent methyl groups appear as a sharp doublet at 0.61 ppm. The spectrum of **35a** is similar and is reported in the Experimental Section.

Though no *tert*-butyl ethylene complex is observed by NMR spectroscopy at low temperature, the isobutyl ethylene complex may still be in equilibrium with a small amount of this 3° alkyl ethylene species. To investigate whether any migratory insertion of ethylene into the *tert*-butyl-Pd bond occurs, the isobutyl ethylene complexes **35a,b** were generated in situ on a preparatory scale and allowed to undergo migratory insertion at −20 °C for 10 min (ca. 1 half-life) (Scheme 13).

Scheme 13. Comparison of 1° vs 3° Butyl Migration Rates Determined by GC

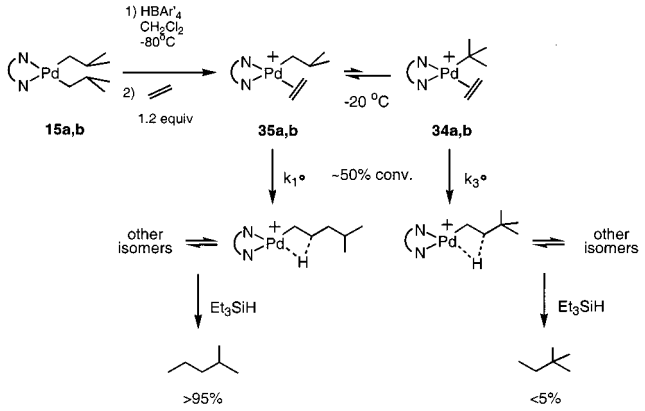

The reaction was quenched by the addition of excess Et_3SiH, which cleaves the alkyl chain from the Pd center, liberating the corresponding alkane. Thus, insertion of ethylene into the Pd−isobutyl bond of **35a,b** would produce 2-methylpentane; insertion of ethylene into the Pd−*tert*-butyl bond of **34a,b** would produce 2,2-dimethylbutane. The volatile organics were vacuum transferred away from the Pd residue and analyzed by GC. Only 2-methylpentane was observed. No 2,2-dimethylbutane was detected (<5%) from either **34a** or **34b**, indicating that little to no insertion occurs into 3° alkyl−Pd bonds in this system. This observation is consistent with branching analyses for polyethylenes produced from (α-diimine)Pd catalysts.[23]

The lack of insertion into Pd−*tert*-butyl bonds indicates that all insertion in **35a,b** occurs via the isobutyl ethylene species, allowing quantification of insertion rates using NMR spectroscopy. In the presence of 20 equiv of ethylene, monitoring the loss of the isobutyl methyl groups in **35a,b** with respect to time yields $k = 6.5(0.1) \times 10^{-4}$ s^{-1} at −17 °C for **35a**, corresponding to $\Delta G^{\ddagger} = 18.7 \pm 0.1$ kcal/mol, and $k = 8.5(0.2) \times 10^{-4}$ s^{-1} at −22 °C for **35b**, corresponding to $\Delta G^{\ddagger} = 18.1 \pm 0.1$ kcal/mol.

(α-Diimine)Pd(CH(CH$_3$)(CH$_2$CH$_3$))(CH$_2$═CH$_2$)$^+$ and (α-Diimine)Pd((CH$_2$)$_3$CH$_3$)(CH$_2$═CH$_2$)$^+$ Complexes. When ethylene is added to CD_2Cl_2 solutions of the agostic *sec*-butyl complexes **28a,b** at −78 °C, isomerization to the *n*-butyl ethylene cations is observed by ^{1}H NMR spectroscopy. In an attempt to observe the kinetic product of ethylene trapping, ethylene was added via syringe to a $CDCl_2F$ solution of **28b** at ca. −130 °C in a pentane/N_2 bath. At −90 °C, the ^{1}H NMR spectrum of this sample reveals trapping and formation of the *sec*-butyl ethylene complex, **36b** (eq 12).

The acenaphthyl *para* protons of **36b** appear as doublets at 8.01 and 7.97 ppm; the *ortho* protons also appear as doublets, at 6.50 and 6.37 ppm. Bound ethylene is observed as second-order multiplet centered at 4.64 ppm. This is likely due to the chiral center at C_α of the *sec*-butyl group, which, even in the regime of rapid ethylene rotation, creates two distinct sets of ethylene protons. The methine proton of the Pd−*sec*-butyl group resonates at 2.05 ppm; one methyl group appears as a doublet at 0.70 ppm, while the other appears as a multiplet at 0.36 ppm (the methylene group is obscured). The absence of (α-diimine)-Pd((CH$_2$)$_3$CH$_3$)(CH$_2$═CH$_2$)$^+$, **37b**, is further indication of the

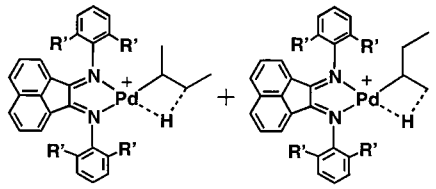

R' = Me (**28a**), iPr (**28b**)

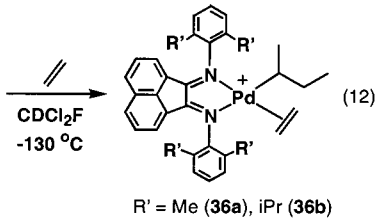

R' = Me (**36a**), iPr (**36b**)

(12)

absence of **21** in the equilibrium mixture of Pd−butyl complexes (see Scheme 8). When **36b** is warmed to −50 °C, the *sec*-butyl ethylene complex isomerizes rapidly to the *n*-butyl ethylene complex, **37b**. The acenaphthyl *para* protons for this species appear as doublets at 8.07 and 8.03 ppm; the *ortho* protons appear at 6.59 and 6.55 ppm. Bound ethylene appears as a sharp singlet at 4.68 ppm, while resonances for the *n*-butyl group appear at 1.56 (α-CH_2), 0.97 (γ-CH_2), and 0.58 (CH_3); the β-CH_2 is obscured. Integration of the acenaphthyl ortho protons of **37b** with respect to those of the *sec*-butyl ethylene complex **36b** yields an equilibrium constant K_{eq} = 125 at −50 °C (eq 13).

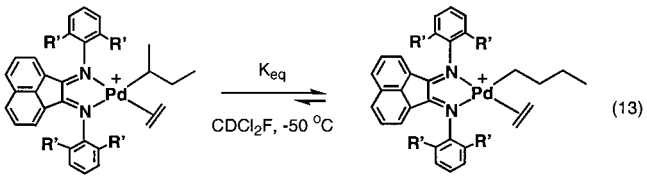

R' = Me (**36a**), iPr (**36b**) R' = Me (**37a**), iPr (**37b**)

K_{eq} = 50 (**36a/37a**)

K_{eq} = 125 (**36b/37b**)

(13)

The case is similar for the *sec*-butyl ethylene/*n*-butyl ethylene complexes **36a/37a**, except that K_{eq} for this system is 50 at −50 °C, reflecting decreased steric interaction in the *sec*-butyl complex.

With the equilibrium constants for the *sec*-butyl/*n*-butyl ethylene complexes in hand, GC experiments similar to those done in the *tert*-butyl/isobutyl ethylene case were carried out to determine the rate of insertion into 2° alkyl centers relative to insertion into 1° alkyl centers. Mixtures of the *sec*-butyl ethylene and *n*-butyl ethylene complexes were generated in situ (preparatory scale) by addition of ca. 1 equiv of ethylene to the isolated agostic salts **28a,b** dissolved in CH_2Cl_2 at −78 °C. The mixtures were warmed to −20 °C for 10 min and then quenched by addition of excess Et_3SiH. Insertion into the Pd−*n*-butyl bond in **37** produces *n*-hexane after silane quenching, while insertion into the Pd−*sec*-butyl bond in **36** produces 3-methylpentane. Volatiles products were vacuum transferred and analyzed by GC; the ratio of *n*-hexane to 3-methylpentane for **36a/37a** was 9.3, while the ratio for **36b/37b** was 6.7 (Scheme 14).

GC analysis also revealed a significant amount of *n*-butane, indicating that not all of the butyl complexes had undergone insertion. A negligible amount of *n*-octane was observed, resulting from double ethylene insertion, indicating that the *n*-hexane/3-methylpentane ratios were not skewed by differential

Scheme 14. Comparison of 1° vs 2° Butyl Migration Rates, As Determined by GC Experiments

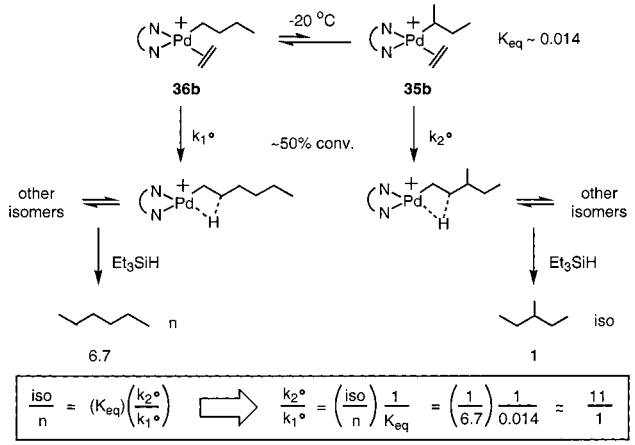

Scheme 15. Comparison of 1° vs 2° Propyl Migration Rates, as Determined by GC

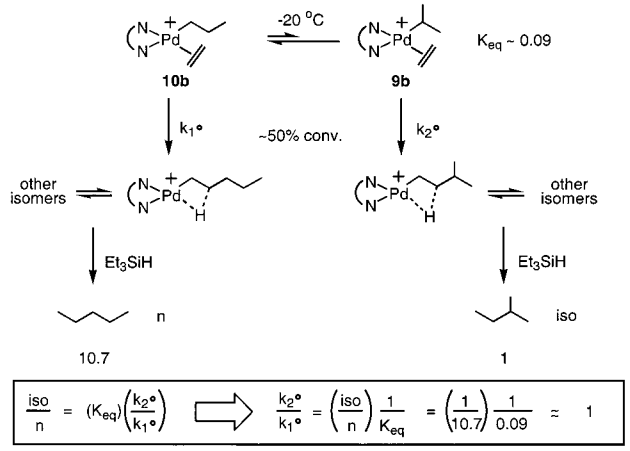

rates of insertion of a second 1 equiv of ethylene. Indeed, the *n*-hexane/3-methylpentane ratio remained invariant though somewhat different amounts of octane were observed for different runs. Clearly Curtin−Hammett conditions apply (equilibrium is rapid, and insertion is rate determining),[48,49] and after extrapolation of the applicable equilibrium constants to −20 °C (assuming ΔS ca. 0), ratios for $k(2°)/k(1°)$ of ca. 2/1 for **36a/37a** and ca. 11/1 for **36b/37b** are obtained.

(α-Diimine)Pd(propyl)(CH_2=CH_2)$^+$ Complexes. The propyl ethylene complexes **9b** and **10b** were generated by addition of ethylene to the isopropyl agostic cation **7b** and have been previously characterized.[22] GC experiments identical to those discussed above were done using an in-situ-generated mixture of the isopropyl ethylene complex **9b** and the *n*-propyl ethylene complex **10b** (Scheme 15).

Analysis of the volatile products after quenching and vacuum transfer revealed a ratio of *n*-pentane to 2-methylbutane of 10.7. Using an extrapolated K_{eq} of 0.09 at −20 °C (K_{eq} = 0.05 at −50 °C), the ratio of $k(2°)/k(1°)$ is calculated to be ca. 1 for **9b/10b**.

Discussion

Dynamics and Relative Stabilities of Agostic Pd(alkyl)$^+$ Cations. The relative stabilities of agostic (α-diimine)Pd(butyl)$^+$ complexes reported here support the trend initially noted for

(48) Seeman, J. I. *Chem. Rev.* **1983**, *83*, 83−134.
(49) Zefirov, N. S. *Tetrahedron* **1977**, *33*, 2719−2722.

Scheme 16. Dynamic Processes for Agostic Ethyl Complex **11b**

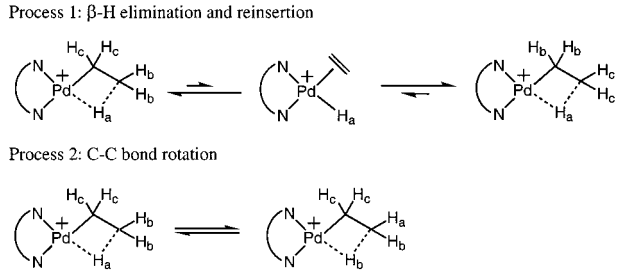

the isopropyl and *n*-propyl complexes, namely, that alkyl substitution is preferred at C_α relative to C_β. This unexpected trend[50] is most dramatic for the *tert*-butyl system, in which the β-agostic Pd(*tert*-butyl)$^+$ isomers, **18a,b**, are much more stable than the Pd(isobutyl)$^+$ isomers, **17a,b**. In the case of the linear butyl isomers, the agostic Pd(*n*-butyl)$^+$ system, **21a,b**, bearing an ethyl substituent at C_β, is disfavored relative to *sec*-butyl isomers **20a,b**, which bear ethyl groups at C_α, a situation analogous to the isopropyl versus *n*-propyl system. In this butyl system, however, the cis and trans *sec*-butyl isomers, **19a,b**-*cis* and **19a,b**-*trans*, bearing single methyl substituents at both C_α and C_β, are favored. Since the C_α–C_β bond exhibits partial double-bond character, the greater stability of these isomers could be rationalized on the basis of analogy with relative alkene stabilities (2-butenes are more stable than 1-butene). The preference for substituents to reside at C_α relative to C_β appears to be electronic in origin and has been addressed by Ziegler using DFT calculations (see below).

The fact that the *sec*-butyl isomers **19a,b** are favored over **20a,b** suggests that in the polymerization system the preferred Pd(alkyl)$^+$ isomers will be those in which Pd resides in positions such that both C_α and C_β bear substituents.

The dynamics of the cationic alkyl complexes are also important to consider due to their intermediacy in isomerization of the alkyl ethylene complexes. Studies of the ethyl agostic complex **11b** indicate that the barrier to β-H elimination is 7.1 kcal/mol ($\Delta G^\ddagger$, −108 °C), while the barrier to rotation of the C_α–C_β bond is ca. 8.4 kcal/mol (Scheme 16).[18]

The barrier to Pd−C_α rotation cannot be measured using this complex but can be quantified in the isopropyl agostic cation **7b**; measurement of the barrier to interconversion of the two isopropyl methyl groups gives a Pd−C_α bond rotation barrier of 9.6 kcal/mol.[21] The barrier to rotation of the C_α–C_β bond in this species is 9.2 kcal/mol, consistent with the fact that methyl group rotation in **7b** develops an eclipsing interaction between a C−H bond of the rotating methyl group and the methyl substituent on C_α (Figure 7).

The butyl complexes **19**−**21** serve to illustrate the barriers involved in Pd migration along the backbone of a hydrocarbon chain during polymerization (Scheme 17).

In order for Pd to walk from C1 to C2, β-H elimination and reinsertion must occur, with a barrier of ca. 7−8 kcal/mol. (The identity of the agostic hydrogen remains fixed throughout this process.) For Pd to move to C3, however, the agostic interaction must be released, Pd−C2 bond rotation must occur, and a new agostic interaction must be formed; then β-H elimination and reinsertion can occur, moving Pd to C3. The rate-determining

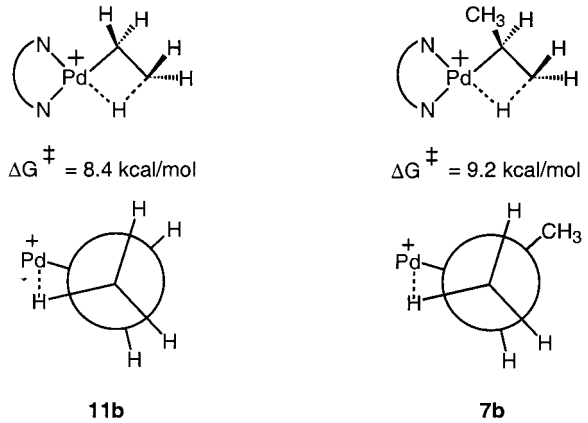

Figure 7. C−C bond rotation in agostic ethyl (**11b**) and isopropyl (**7b**) complexes.

Scheme 17. Isomerization of Pd(alkyl)$^+$ Complexes via β-H Elimination and Bond Rotation

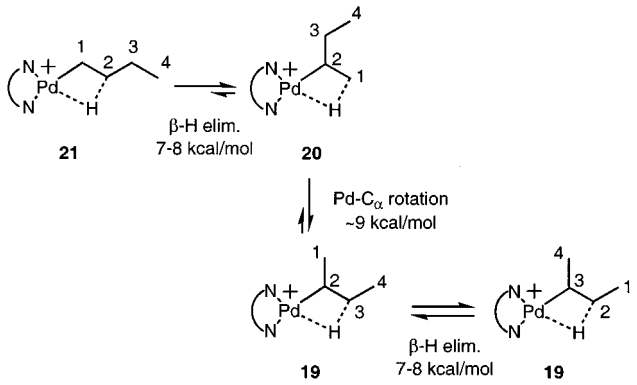

step for this process is likely Pd−C bond rotation, as this barrier was measured to be ca. 9.6 kcal/mol in the isopropyl system. Thus, the barrier to Pd migration along the polymer chain involves not only β-H elimination but also rotation around the Pd−C_α bond, which is the higher barrier.

The observation of a stable, thermodynamically favored agostic *tert*-butyl complex is also of key significance. To migrate back and forth through a branch point on the polymer backbone and to migrate onto branches themselves, the Pd center must be able to pass easily through 3° alkyl centers. The high stability of the *tert*-butyl complexes (**18a,b**) shows that formation of a Pd−tertiary alkyl species poses no barrier to migration through a branch point in the polymer.

Equilibria in (α-Diimine)Pd(alkyl)(CH_2═CH_2)$^+$ Complexes. The trend observed for the alkyl ethylene complexes is opposite that seen in the agostic alkyl complexes: 1° alkyl ethylene complexes are favored over 2° alkyl ethylene complexes and 3° alkyl ethylene complexes (specifically, the Pd(*tert*-butyl)(CH_2═CH_2)$^+$ complex). This thermodynamic preference is likely steric in nature: the η^2-bound olefin adds significant steric bulk to the fourth coordination site relative to the β-C−H agostic interaction and favors isomerization of the alkyl group to the least sterically demanding species. This is supported by the observation that the *n*-alkyl ethylene cations are more heavily favored (*n*-butyl/*sec*-butyl = 125 for **37b**/**36b** at −50 °C) when the imine aryl rings bear isopropyl groups than when they bear less bulky methyl groups (*n*-butyl/*sec*-butyl = 50 for **37a**/**36a** at −50 °C).

Secondary alkyl ethylene complexes such as the isopropyl ethylene species **9b** and the *sec*-butyl ethylene species **36a,b** can be observed as the kinetic products of trapping the

(50) Primary alkyl metal complexes are generally thought to be more stable than secondary and tertiary ones; steric factors are regarded as responsible for this trend. See: Collman, J. P.; Hegedus, L. S.; Norton, J. R.; Finke, R. G. *Principles and Applications of Organotransition Metal Chemistry*. University Science: Mill Valley, CA, 1987; p 99.

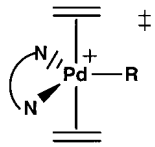

Figure 8. Probable 5-coordinate transition state for associative exchange of ethylene.

corresponding alkyl agostic cations with ethylene at low temperature. Upon warming, these species isomerize to the thermodynamically favored *n*-alkyl complexes. Experiments with the ethyl ethylene cation **30b** indicate that this isomerization occurs via initial loss of ethylene, with a barrier of 17.1 kcal/mol for ethylene dissociation. The overall isomerization barrier for the isopropyl ethylene complex **9b** has been measured as 15.3 kcal/mol (see Figure 2). This indicates that the barrier to dissociation of ethylene from the isopropyl species is at a minimum 1.8 kcal/mol lower than the barrier measured in the ethyl ethylene case. This lower barrier can be ascribed to more crowding in the square plane of the 2° alkyl ethylene species relative to the 1° alkyl species. The barrier to ethylene dissociation for the ethyl ethylene cation **30b** can be compared to the barrier to insertion of ethylene in the same species. The migratory insertion barrier is 1.4 kcal/mol more than that for dissociation of ethylene for the case of a 1° alkyl ethylene species, which indicates that Pd can migrate across many carbons on the polymer chain before undergoing an insertion event.

Associative Exchange Rates. Although alkyl olefin isomerization occurs via loss of olefin, associative exchange rates measured for the ethyl ethylene complexes **30a,b** indicate that bound ethylene undergoes *associative* exchange with free ethylene at rates much higher than rates for dissociative ethylene loss (even at low ethylene concentrations). For example, at $[C_2H_4] = 10$ mM, the rate ratio of associative loss versus dissociative loss is ca. 10^8:1 at −85 °C. The associative exchange rates measured for these species track well with those measured for the analogous methyl ethylene complexes (Table 2) in that addition of bulk to the ortho positions on the imine aryl rings slows associative exchange. Experiments with the ethyl ethylene complexes indicate that addition of bulk in the square plane of the complex (i.e. ethyl rather than methyl) *increases* the rate of ethylene exchange. Associative exchange of ethylene in these systems most likely occurs via a 5-coordinate transition state in which the two olefin moieties are in the axial sites (Figure 8).

As noted previously,[9,22] addition of bulk near these axial sites (via an increase the size of the alkyl groups in the ortho positions on the imine aryl rings) should raise the energy of this transition state with respect to the ground-state alkyl olefin complex, raising the barrier to associative exchange as observed. The fact that increasing the size of the Pd alkyl substituent increases the rate of associative exchange suggests that the alkyl group experiences more steric crowding in the square planar ground state than the transition state. If the transition state shown in Figure 8 is a good model for the transition state, reduced crowding may result from widening the N−Pd−R angle.

Primary versus Secondary Alkyl Migratory Insertion Barriers. Prior to this study, average barriers for migratory insertion during polymerization had been obtained using turnover numbers from the methyl ethylene complexes **33a,b**.[22] Those barriers, termed "subsequent insertion" barriers, are shown in Table 3 and are average barriers for migration of all types of 1° and 2° alkyl groups to bound ethylene in these systems. Using the ethyl ethylene cations **30a,b** and isobutyl ethylene cations **35a,b**, barriers for migratory insertion of 1° alkyl ethylene complexes were obtained and are also shown in Table 3 for comparison.

Table 3. Average Insertion Barriers versus 1° Alkyl Insertion Barriers for Cationic (α-diimine)Pd Ethylene Polymerization Catalysts

Pd complex	av insertion (kcal/mol)	1° alkyl insertion (kcal/mol)
30a	18.6	18.9
30b	18.0	18.5
35a	18.6	18.7
35b	18.0	18.1

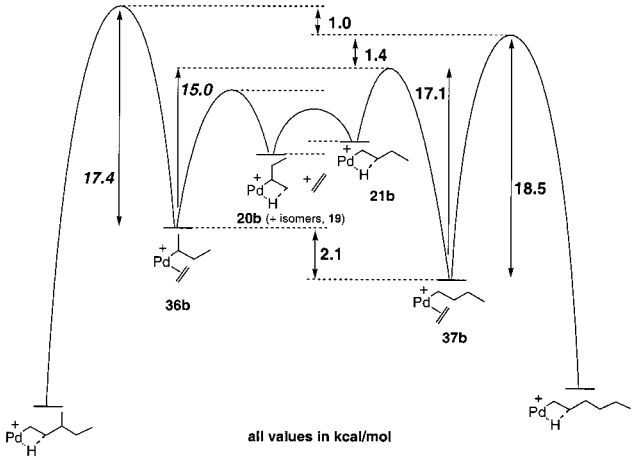

Figure 9. Free energy diagram for insertion and isomerization in **36b**/**37b**.

The barrier to 1° alkyl migratory insertion is higher than the average, significantly so for the *n*-alkyl ethyl ethylene complexes **30a,b**. The data from the isobutyl ethylene cations **35a,b** indicate that the barrier to insertion is slightly higher than the average even when C_β is a tertiary carbon center. Because no insertion occurs from 3° alkyl ethylene species (as indicated by the isobutyl ethylene/*tert*-butyl ethylene GC experiment), the barrier to insertion in 2° alkyl complexes must therefore be lower than the average—in some cases much lower, to counterbalance the higher barrier to insertion in the *n*-alkyl ethylene complexes.

Taking advantage of the Curtin−Hammett kinetic situation and the ability to measure the equilibrium ratio of the Pd(*n*-butyl)(ethylene)$^+$ to Pd(*sec*-butyl)(ethylene)$^+$ complexes, the relative rates of insertion of ethylene into the 1° vs 2° butyl groups could be determined by GC analysis of product ratios as described in the Results. These experiments indicate that the rate of secondary insertion for **36b** is nearly 11 times faster than primary insertion. Reducing the steric bulk on the ligand (**36a**) lowers the $k(2°)/k(1°)$ ratio significantly, to ca. 2 to 1. Less crowding in the case of the 2,6-dimethyl-substituted ligand likely results in lower ground-state energies for these species, raising insertion barriers and decreasing the difference in ground-state energies between the *n*-alkyl and *sec*-alkyl ethylene complexes. This is reflected in the lowering of K_{eq} (*n*-butyl ethylene/*sec*-butyl ethylene) upon changing the ligand aryl substituents from isopropyl groups to methyl groups.

Using data obtained from the ethyl ethylene species to model insertion and ethylene dissociation in the butyl ethylene complexes, the free energy diagram shown in Figure 9 can be constructed for complexes **36b**/**37b**.

NMR spectroscopic data have established that the *sec*-butyl ethylene complex, **36b** in Figure 9, is thermodynamically favored over the agostic *n*-butyl species **37b** by 2.1 kcal/mol.

Using the ethyl ethylene complex **30b** as a model for the butyl ethylene complex **37b**, the barrier to dissociation of ethylene (and thus to isomerization from *n*-butyl to *sec*-butyl) can be estimated as 17.1 kcal/mol; this is 1.4 kcal/mol lower than the barrier to migratory insertion (18.5 kcal/mol), which is also estimated from the results for **30b**. GC product ratios from insertion of ethylene in **36b**/**37b** allow calculation of $\Delta\Delta G^{\ddagger} =$ 1.0 kcal/mol for the difference in the overall barriers to product formation (Curtin−Hammett kinetics apply). With these pieces of information in hand, the barriers to *sec*-butyl ethylene isomerization and migratory insertion can be deduced. The barrier to isomerization of **36b** to **37b** is 17.1 − 2.1 = 15.0 kcal/mol; this compares well with the barrier to 2° alkyl olefin isomerization of 15.3 kcal/mol measured for the transformation of the isopropyl ethylene complex **9b** to the *n*-propyl ethylene complex **10b**.[22] The barrier to 1° alkyl olefin insertion plus the overall difference in barriers to product formation (18.5 + 0.9 = 19.4 kcal/mol) minus the difference in free energy between **36b** and **37b** then gives an estimate of the barrier to migratory insertion for a 2° alkyl olefin species, 19.4 − 2.1 = 17.3 kcal/mol. The magnitude of this barrier indicates that 2° alkyl migratory insertion is almost 10 times faster than 1° alkyl migratory insertion at −20 °C, likely due to crowding in the ground state of **36b**. This much lower barrier to 2° alkyl migratory insertion is necessary to observe a high degree of branching in the resulting polymer, considering that the *n*-alkyl ethylene complexes are the most likely catalyst resting states.

Comparison to Theoretical Results. Ziegler et al. have reported extensive density functional calculations on the Ni[47,51] and Pd[37,38] catalyst systems. Using a generic α-diimine ligand, Ziegler calculates that the Pd agostic isopropyl cation (**38**, R, R′ = H, CH_3) should be favored over the Pd *n*-propyl cation (**39**, R, R′ = H, CH_3) by 1.96 kcal/mol, and the agostic *tert*-butyl cation (**38**, R, R′ = CH_3, CH_3) should be heavily favored thermodynamically (by 3.42 kcal/mol over the isobutyl cation, **39**, R, R′ = CH_3, CH_3) (eq 14).[37]

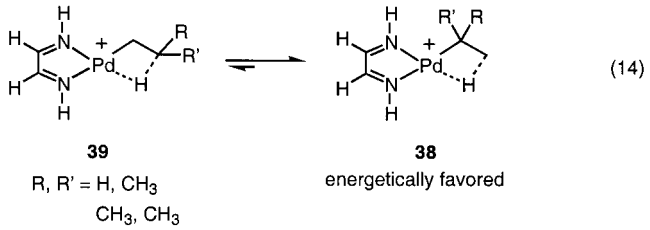

(14)

The *sec*-butyl cations (**41** and **42**) are also calculated to be more stable than the *n*-butyl agostic cation **40** by almost 3 kcal/mol, with the *sec*-butyl cation having a methyl branch on C_α (**42**) being the more favored of the two *sec*-butyl cations by 1.24 kcal/mol (eq 15).

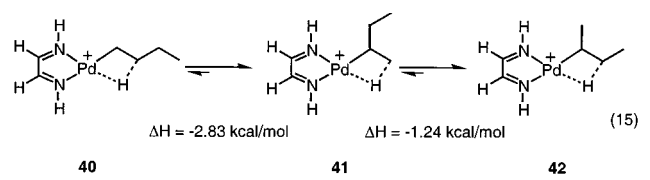

(15)

All of these calculated ground state energies are in good agreement with the relative energy ordering of the actual propyl and butyl agostic cations described in this work. The fact that the model imine ligand bears no bulky aryl substituents and the calculated ordering matches that observed experimentally suggests that electronic effects are the largest factor controlling relative agostic alkyl stabilities.

Use of the generic α-diimine ligand is less satisfactory for predicting relative stabilities of the alkyl ethylene complexes and their insertion barriers. The 1° alkyl ethylene cations are calculated to be only slightly more stable (by 0.64 kcal/mol) relative to the isomeric 2° alkyl ethylene species, and the lowest insertion barrier calculated is that into a Pd−1° alkyl bond (lower than into the Pd−2° alkyl bond by 1.32 kcal/mol).[37] This insertion barrier, calculated for an *n*-propyl ethylene cation, is 18.83 kcal/mol, very close to our measured insertion barriers in the actual catalyst system.[22]

Changing the diimine backbone to acenaphthyl and the imine substituents to 2,6-(^{i}Pr)$_2$C$_6$H$_3$ in the calculation shows an enhanced preference for the 2° alkyl agostic cations; the isopropyl cation **7b** is calculated to be more stable than the *n*-propyl cation **9b** by 2.65 kcal/mol. The *n*-alkyl ethylene complexes also become much more stable relative to 2° alkyl ethylene complexes; for example, the *n*-propyl ethylene complex **10b** is favored over the isopropyl ethylene complex **9b** by 2.01 kcal/mol.[38] These results using the actual ligand set suggest that the observed preference for the *n*-alkyl ethylene complexes is steric rather than electronic in nature.

Summary and Conclusions

Cationic (α-diimine)Pd(II) alkyl species are intermediates in the polymerization of ethylene and α-olefins to high molecular weight polyolefins. These *β*-agostic alkyl complexes have been synthesized independently via protonation of (α-diimine)Pd dialkyl complexes, which has allowed study of their structures, dynamic behavior, and the equilibria between isomeric species. Addition of ethylene to these cations produces alkyl ethylene complexes and provides a means of investigation of the equilibria and rates of migratory insertion for these resting state species. Studies of (α-diimine)Pd−ethyl, −propyl, −*n*-butyl, and −isobutyl agostic complexes and their corresponding ethylene complexes have yielded new mechanistic information about these diimine Pd(II) polymerization catalysts. Key findings are as follows:

(1) The most stable isomeric agostic Pd alkyl cation is that having the highest degree of substitution at C_α. For example, the Pd *tert*-butyl cation is favored over the isobutyl complex, and the Pd isopropyl cation is favored over the isomeric Pd *n*-propyl complex. In the case of the *n*-butyl system, the thermodynamically favored isomers are those with methyl substituents at both C_α and C_β. Electronic effects appear to govern these equilibria.

(2) Addition of ethylene to the agostic alkyl complexes results in trapping as the alkyl ethylene complexes, which can equilibrate via Pd chain walking prior to insertion. Here, the opposite trend in relative stabilities is observed: 1° alkyl ethylene species are heavily favored over 2° alkyl ethylene complexes, and no 3° alkyl ethylene complexes have been observed. These relative stabilities appear to be controlled by steric effects.

(3) The kinetic products of ethylene trapping of 2° alkyl agostic species are the more sterically demanding 2° alkyl ethylene complexes. However, these species isomerize rapidly to the 1° alkyl ethylene species via a mechanism that involves initial dissociation of ethylene, isomerization of the resulting alkyl agostic cation, and reassociation of ethylene. The barrier to dissociation of ethylene in 1° alkyl ethylene cations (modeled with an ethyl ethylene species) is 1.4 kcal/mol less than the

(51) Deng, L.; Woo, T. K.; Cavallo, L.; Margl, P. M.; Ziegler, T. *J. Am. Chem. Soc.* **1997**, *119*, 6177−6186.

corresponding migratory insertion barrier. The barrier to ethylene dissociation in 2° alkyl ethylene species is estimated at 15.0 kcal/mol, almost 3 kcal/mol lower than insertion. This finding confirms that ethylene loss and alkyl isomerization are facile processes compared to chain propagation via insertion and result in formation of highly branched polyethylene.

(4) The alkyl ethylene complexes undergo associative exchange of bound ethylene with free ethylene in solution. Increasing the steric bulk of the imine aryl substituents slows the rate of associative exchange, while increasing the bulk of the Pd−alkyl chain (−CH_3 vs −CH_2CH_3) slightly increases the exchange rate.

(5) No migratory insertion is observed to occur through 3° alkyl ethylene species, consistent with established branching patterns in the polymers produced from the Pd catalysts.[23]

(6) The rate of migratory insertion of 2° alkyl ethylene complexes is generally faster than that for 1° alkyl ethylene complexes. For the bulkier system bearing aryl substituents with *ortho* isopropyl groups (series **b**), the 2°:1° ratio is 11:1 (−20 °C), whereas for the less bulky system bearing *ortho* methyl groups (series **a**) this rate ratio falls to 2:1 (−20 °C). The ground state energy of a secondary alkyl ethylene complex relative to a primary alkyl ethylene complex is apparently raised more through steric interactions in the case of the isopropyl-substituted catalyst than in the case of the less bulky methyl-substituted catalyst. On this basis, it might be anticipated that the methyl-substituted catalyst system would yield polyethylene with fewer branches (i.e., more chain propagation would occur through migratory insertions of 1° alkyl ethylene complexes which produce no branch). However, alkyl olefin complexes equilibrate prior to insertion, and these 1° vs 2° rate differentials for insertion are nearly exactly counterbalanced by a greater thermodynamic preference for 2° alkyl ethylene complexes in the case of the *ortho* methyl-substituted system relative to the *ortho* isopropyl-substituted system. Thus, similar degrees of branching of the polyethylenes produced from the two catalyst systems are observed.[52] At the single insertion level, this is illustrated in Scheme 14, where the ratios of *n*-hexane (linear) to 3-methylpentane (branched) generated from insertion and cleavage of the equilibrating (α-diimine)Pd(butyl)(ethylene)$^+$ isomers are nearly within experimental error for the two catalyst systems.

Experimental Section

General Considerations. All manipulations of compounds were performed using standard high-vacuum or Schlenk techniques. Argon was purified by passage through columns of BASF R3-11 catalyst (Chemalog) and 4 Å molecular sieves. Solid organometallic compounds were transferred in an argon-filled MBraun drybox. NMR spectra were acquired with Bruker DRX400 or DRX500 spectrometers. NMR probe temperatures were measured using an Omega type T thermocouple immersed in anhydrous methanol in a 5 mm NMR tube. ^{1}H and ^{13}C chemical shifts are reported in ppm downfield of TMS and were referenced to residual ^{1}H NMR signals and to the ^{13}C NMR signals of the deuterated solvents, respectively. All coupling constants are reported in Hz. Elemental analyses were performed by Atlantic Microlab, Inc., of Norcross, GA.

Activation parameters ($\Delta G^{\ddagger}$) were calculated from measured rate constants and temperatures using the Eyring equation. Error analysis of $\Delta G^{\ddagger}$ obtained for dynamic processes was based on Binsch's derivation of $\sigma\Delta G^{\ddagger}$ and incorporated an estimate of 10% error in k and ±1 °C error in temperature.[53] Error calculations for coalescence data incorporated a larger ±5 °C error in the calculation.

Materials. All solvents were deoxygenated and dried via passage over a column of activated alumina.[54] Dichlorofluoromethane-*d* ($CDCl_2F$) was prepared according to the literature,[55] dried over $CaCl_2$, degassed by repeated freeze−pump−thaw cycles, vacuum-transferred, and stored over 4 Å molecular sieves at −30 °C under argon. Methylene chloride-d_2 was dried over P_2O_5, degassed by repeated freeze−pump−thaw cycles, vacuum-transferred, and stored over 4 Å molecular sieves under argon. The α-diimine ligands,[56] $(PhCN)_2PdCl_2$,[57] and $H(OEt_2)_2BAr'_4$,[41] were prepared as previously reported. $NaBAr'_4$ (Ar′ = 3,5-$(CF_3)_2C_6H_3$) (Boulder Scientific) and $B(C_6F_5)_3$ (Strem) were stored in an argon-filled drybox and used as received. *n*-PrMgCl, *n*-BuMgCl, and *i*-BuMgCl were purchased from Aldrich and stored at −30 °C. Ethylene and propylene (CP grade) were purchased from National Welder's Supply Co., Inc. and used without further purification. The synthesis and characterization of the dichloride complexes **12a,b**, the diethyl complexes **31a,b**, the ethyl ether complexes **29a,b**, and the agostic ethyl complex **11b** have been reported.[18]

Synthesis of Dialkyl Complexes. ((2,6-$(CH_3)_2C_6H_3$)N═C(An)C(An)═N(2,6-$(CH_3)_2C_6H_3$))Pd(*n*-C_3H_7)$_2$ (13a). A clean, flame-dried Schlenk flask was charged with ((2,6-$(CH_3)_2C_6H_3$)N═C(An)C(An)═N(2,6-$(CH_3)_2C_6H_3$))$PdCl_2$ (**12a**) (0.435 g, 0.769 mmol) in an argon-filled drybox. The flask was placed under argon and cooled to −78 °C (dry ice/isopropyl alcohol), and Et_2O (20 mL) was added via syringe. *n*-PrMgCl was added as a solution in Et_2O (2.0 M, 0.77 mL, 1.54 mmol) via syringe, and the mixture was stirred at −78 °C for 2 h (the orange suspension gradually changed to dark brown). MeOH (0.1 mL) was added via syringe to quench any excess Grignard reagent, and the dark mixture was cannulated onto Florisil and flash-filtered into a clean, flame-dried Schlenk flask at 0 °C. The Florisil was extracted with Et_2O (1 × 10 mL) and pentane (1 × 10 mL), and the filtrate was reduced in vacuo to give a red-brown foamy solid, which was dried under reduced pressure for 1 h at 25 °C and stored at −30 °C in the drybox freezer. Yield: 0.203 g (45%). ^{1}H NMR (CD_2Cl_2, 400 MHz, 25 °C): δ 8.04 (d, J = 8.3, 2H, An *p-H*), 7.42 (dd, J = 7.3, 8.3, 2H, An *m-H*), 7.26 (m, 6H, Ar *H*), 6.71 (d, J = 7.3, 2H, An *o-H*), 2.26 (s, 12H, ArCH_3), 1.18 (tq, J = 7.2, 7.4, 4H, Pd$CH_2CH_2CH_3$), 0.89 (t, J = 7.4, 4H, PdCH_2-CH_2CH_3), 0.68 (t, J = 7.2, 6H, Pd$CH_2CH_2CH_3$). ^{13}C NMR (CD_2Cl_2, 125 MHz, −50 °C): δ 166.6, 144.5, 142.4, 130.8, 129.8, 128.8, 128.0, 127.5, 125.5, 122.7, 24.2 (Pd$CH_2CH_2CH_3$), 21.9 (Pd$CH_2CH_2CH_3$), 19.3 (Pd$CH_2CH_2CH_3$), 17.7 (Ar-CH_3). Anal. Calcd for $C_{34}H_{38}N_2Pd$: C, 70.27; H, 6.59; N, 4.82. Found: C, 70.50; H, 6.53; N, 4.96.

Compounds **13b**, **14a,b**, and **15a,b** were prepared in an analogous fashion to **13a**. All give satisfactory analyses; experimental details and spectral characterization appear in the Supporting Information.

Synthesis of Agostic Butyl Complexes. [((2,6-$(CH_3)_2C_6H_3$)N═C(An)C(An)═N(2,6-$(CH_3)_2C_6H_3$))Pd(C_4H_9)]BAr'_4 (28a). A clean, flame-dried Schlenk flask was charged with ((2,6-$(CH_3)_2C_6H_3$)N═C(An)C(An)═N(2,6-$(CH_3)_2C_6H_3$))Pd(C_4H_9)$_2$ (**14a**) (50.3 mg, 82.6 μmol) and $H(OEt_2)_2BAr'_4$ (84.3 mg, 83.3 μmol) in an argon-filled drybox. The flask was placed under argon and cooled to −78 °C (dry ice/isopropyl alcohol), and CH_2Cl_2 (5.6 mL) was added via syringe. The solids dissolved immediately to give a yellow-orange solution. The solution was allowed to stir at −78 °C for 20 min; it was then warmed to 0 °C and reduced in vacuo to a yellow-orange powder, which was dried under reduced pressure for 2 h at 25 °C. The product is a mixture of isomers; see the text for details. Yield: 95.0 mg (81%). Ligand resonances for the isomers are coincident and are reported as if the complex were a single species. ^{1}H NMR ($CDCl_2F$, 400 MHz, −110 °C (static)): δ 8.11 (m, 2H, An *p-H*), 7.79 (br s, 8H, BAr'_4 *o-H*), 7.51 (br s, 4H, BAr'_4 *p-H*), 7.31 (m, 8H, An *m-H*, Ar *H*), 6.80 (m, 2H, An *o-H*), 2.25 (m, 12H, ArCH_3). Trans isomer: 1.72 (br m, 1H, Pd(CH(CH_3)C*H*-μ-H(CH_3)), −7.98 (br d, J = 13, 1H, Pd(CH(CH_3)CH-μ-*H*(CH_3)), Pd(C*H*(CH_3)CH-μ-H(CH_3)) obscured. Cis isomer: 1.44 (br m, 2H, Pd(C*H*(CH_3)C*H*-μ-H(CH_3)), −8.10 (br m, 1H, Pd(CH(CH_3)CH-μ-

(52) Gottfried, A. C.; Brookhart, M. Unpublished results.
(53) Binsch, G. In *Dynamic Nuclear Magnetic Resonance Spectroscopy*; Jackman, L., Cotton, F. A., Eds.; Academic Press: New York, 1975; p 77.
(54) Pangborn, A. B.; Giardello, M. A.; Grubbs, R. H.; Rosen, R. K.; Timmers, F. J. *Organometallics* **1996**, *15*, 1518−1520.
(55) Siegel, J. S.; Anet, F. A. L. *J. Org. Chem.* **1988**, *53*, 2629−2630.
(56) van Koten, G.; Vrieze, K. *Adv. Organomet. Chem.* **1982**, *21*, 151−239.
(57) Kharasch, M. S.; Seyler, R. C.; Mayo, F. R. *J. Am. Chem. Soc.* **1938**, *60*, 882−884.

H(CH_3)), Pd(CH(C*H*$_3$)CH-μ-H(C*H*$_3$)) obscured. ^{1}H NMR ($CDCl_2F$, 400 MHz, 0 °C (dynamic)): δ 8.10 (d, J = 8.4, 1H, An *p-H*), 8.07 (d, J = 8.0, 1H, An *p-H*′), 7.71 (br s, 8H, BAr′$_4$ *o-H*), 7.50 (m, 2H, An *m-H*), 7.47 (br s, 4H, BAr′$_4$ *p-H*), 7.27 (m, 6H, Ar *H*), 6.81 (d, J = 7.6, 1H, An *o-H*), 6.79 (d, J = 7.6, 1H, An *o-H*′), 2.26 and 2.24 (2 s, 6H each, ArC*H*$_3$), all Pd−butyl resonances broadened into baseline by exchange. ^{13}C NMR ($CDCl_2F$, 100 MHz, 0 °C): δ 161.7 (q, $^1J_{CB}$ = 49.7, BAr′$_4$ C_{ipso}), 131.56, 134.6 (BAr′$_4$ C_{ortho}), 129.86, 129.62, 129.25 (q, $^2J_{CF}$ = 28.3, BAr′$_4$ C_{meta}), 128.02, 127.74, 127.29, 125.43, 125.38, 125.22, 124.41 (q, $^1J_{CF}$ = 272, BAr′$_4$ CF_3), 117.5 (BAr′$_4$ C_{para}), 31.85, 25.05, 22.81, 18.56, 18.38, 17.94 (Ar*C*H$_3$), 17.63 (Ar*C*′H$_3$), 15.08, 13.98, 13.70. Not all carbons were accounted for. Anal. Calcd for $C_{64}H_{45}N_2BF_{24}$Pd: C, 54.31; H, 3.21; N, 1.98. Found: C, 54.47; H, 3.43; N, 1.96.

[((2,6-(*i*-Pr)$_2$C$_6$H$_3$)N═C(An)C(An)═N(2,6-(*i*-Pr)$_2$C$_6$H$_3$))Pd(C$_4$H$_9$)]-BAr′$_4$ (28b). A procedure identical to that used for **28a** was followed, using ((2,6-(*i*-Pr)$_2$C$_6$H$_3$)N═C(An)C(An)═N(2,6-(*i*-Pr)$_2$C$_6$H$_3$))Pd(C$_4$H$_9$)$_2$ (**14b**) (100 mg, 0.139 mmol) and H(OEt$_2$)$_2$BAr′$_4$ (143 mg, 0.414 mmol) in CH_2Cl_2 (10 mL). Yield: 176 mg (83%) of a yellow-orange powder. The product is a mixture of isomers; see the text for details. Ligand resonances for the isomers are coincident and are reported as if the complex were a single species. ^{1}H NMR ($CDCl_2F$, 400 MHz, −110 °C (static)): δ 8.20 (m, 2H, An *p-H*), 7.73 (br s, 8H, BAr′$_4$ *o-H*), 7.61 (m, 2H, An *m-H*), 7.50 (br s, 4H, BAr′$_4$ *p-H*), 7.47 (m, 6H, Ar *H*), 6.93 (m, 1H, An *o-H*), 6.76 (m, 1H, An *o-H*′), 3.40 and 3.32 (2 overlapping septets, J = 6.8 and 6.8, C*H*MeMe′), 3.13 (septet, J = 6.4, C*H*MeMe′), 2.87 (m, C*H*MeMe′),1.28 (br d, 12 H, CH*MeMe*′), 1.01 (br, 6H, C′H*Me*Me′), 0.93 (br, 6H, C′HMe*Me*′). Trans isomer: 1.72 (m, 1H, Pd(CH(CH$_3$)C*H*-μ-H(CH$_3$)), 0.15 (br d, 3H, Pd(CH(CH$_3$)-CH-μ-H(C*H*$_3$)), −8.20 (br d, J = 17, 1H, Pd(CH(CH$_3$)CH-μ-*H*(CH$_3$)), Pd(C*H*(C*H*$_3$)CH-μ-H(CH$_3$)) obscured. Cis isomer: 1.35 (m, 2H, Pd-(C*H*(CH$_3$)C*H*-μ-H(CH$_3$)), −8.27 (t, J = 7, 1H, Pd(CH(CH$_3$)CH-μ-*H*(CH$_3$)), Pd(CH(C*H*$_3$)CH-μ-H(C*H*$_3$)) obscured. *sec*-Butyl agostic isomer with ethyl branch: −8.01 (t, J = 16, 1H, Pd(CH(CH$_2$CH$_3$)CH$_2$-μ-*H*)), Pd(C*H*(C*H*$_2$CH$_3$)C*H*$_2$-μ-H) obscured. ^{1}H NMR ($CDCl_2F$, 400 MHz, 0 °C (dynamic)): δ 8.08 (d, J = 8.4, 1H, An *p-H*), 8.05 (d, J = 8.4, 1H, An *p-H*′), 7.72 (br s, 8H, BAr′$_4$ *o-H*), 7.52 (m, 2H, An *m-H*), 7.49 (br s, 4H, BAr′$_4$ *p-H*), 7.41 (m, 6H, Ar *H*), 6.80 (d, J = 7.6, 1H, An *o-H*), 6.60 (d, J = 7.6, 1H, An *o-H*′), 3.15 (m, 4H, C*H*MeMe′, C′*H*MeMe′), 1.35 (d, J = 6.8, 12 H, CH*MeMe*′), 1.06 (d, J = 6.8, 6H, C′H*Me*Me′), 0.96 (d, J = 6.8, 6H, C′HMe*Me*′), all Pd−butyl resonances broadened into baseline by exchange. ^{13}C NMR ($CDCl_2F$, 100 MHz, 0 °C): δ 161.7 (q, $^1J_{CB}$ = 49.7, BAr′$_4$ C_{ipso}), 151.1, 146.0, 144.2, 142.1, 142.0, 139.3, 138.4, 137.5, 134.6 (BAr′$_4$ C_{ortho}), 133.5, 133.0, 131.7, 130.2, 130.0, 129.25 (q, $^2J_{CF}$ = 28.3, BAr′$_4$ C_{meta}), 128.4, 127.6, 126.3, 125.8, 125.5, 125.3, 125.0, 124.41 (q, $^1J_{CF}$ = 272, BAr′$_4$ CF_3), 117.5 (BAr′$_4$ C_{para}), 31.8, 30.3, 29.8, 29.6, 29.5, 25.0, 24.0, 23.5, 23.4, 23.3, 23.2, 23.0, 22.8, 22.7, 22.3, 14.0, 13.7. Not all carbons were accounted for. Anal. Calcd for $C_{72}H_{61}N_2BF_{24}$Pd: C, 56.61; H, 4.03; N, 1.83. Found: C, 56.75; H, 4.15; N, 1.88.

General Procedures for Variable-Temperature NMR Experiments. In a drybox under an argon atmosphere, a tared NMR tube was charged with ca. 0.01 mmol each of the desired dialkyl complex and H(OEt$_2$)$_2$BAr′$_4$ or ca. 0.01 mmol of the isolated agostic alkyl complex. The tube was capped with a rubber septum in the drybox and secured with Teflon tape and Parafilm once removed from the drybox. The tube was then cooled to −78 °C (dry ice/acetone bath), and CD_2Cl_2 was added via gastight syringe (22-gauge needle, ∼700 μL). Alternatively, $CDCl_2F$ was used for lower temperature work; it was added to the NMR tube via a 22-gauge cannula. The tube was then removed from the bath briefly and shaken to facilitate dissolution of the solids (and subsequent reaction, in the case of the dialkyl complexes). The tube was kept in the bath until it could be transferred to a precooled (−80 °C) NMR probe for acquisition of spectra. The concentrations of all species were calculated using the BAr′$_4$ or acenaphthyl ^{1}H signals (*ortho* or *para*) as internal standards. Acetonitrile was added to the NMR tube via a 10-μL syringe to produce acetonitrile complexes; ethylene was added via a gastight syringe with a 22-gauge needle. CO was bubbled directly through the solution in the NMR tube using a 22-gauge needle.

In Situ Formation of Agostic Alkyl Complexes. With the exception of the agostic butyl complexes, whose synthesis is described in the previous section, agostic alkyl complexes were studied by in situ generation from the corresponding dialkyl complex and H(OEt$_2$)$_2$BAr′$_4$. The byproducts of these reactions (generally an alkane and Et$_2$O) are not included in the NMR data for the species, though they may in some cases obscure resonances from the agostic complexes themselves.

[((2,6-(CH$_3$)$_2$C$_6$H$_3$)N═C(An)C(An)═N(2,6-(CH$_3$)$_2$C$_6$H$_3$))Pd(CH-(CH$_2$-μ-H)(CH$_3$))]BAr′$_4$ (7a). See ref 22 for spectral data.

[((2,6-(*i*-Pr)$_2$C$_6$H$_3$)N═C(An)C(An)═N(2,6-(*i*-Pr)$_2$C$_6$H$_3$))Pd(CH-(CH$_2$- μ-H)(CH$_3$))]BAr′$_4$ (7b). See ref 21 for spectral data.

[((2,6-(CH$_3$)$_2$C$_6$H$_3$)N═C(An)C(An)═N(2,6-(CH$_3$)$_2$C$_6$H$_3$))Pd(C-(CH$_2$- μ-H)(CH$_3$)$_2$)]BAr′$_4$ (18a). ^{1}H NMR ($CDCl_2F$, 400 MHz, −110 °C (static)): δ 8.08 (m, 2H, An *p-H*), 7.77 (br s, 8H, BAr′$_4$ *o-H*), 7.49 (br s, 4H, BAr′$_4$ *p-H*), 7.39−7.22 (m, 8H, An *m-H*, Ar *H*), 6.79 (d, J = 6.8, 1H, An *o-H*), 6.66 (d, J = 7.2, 1H, An *o-H*′), 2.23 and 2.15 (2 s, 6H each, Ar*Me*$_2$, Ar′*Me*$_2$), 0.56 (br s, 6H, Pd(C(CH$_2$-μ-H)(C*H*$_3$)$_2$)), −7.03 (br t, J = 15, 1H, Pd(C(CH$_2$-μ-*H*)(CH$_3$)$_2$), Pd(C(C*H*$_2$-μ-H)-(CH$_3$)$_2$) obscured. ^{1}H NMR ($CDCl_2F$, 400 MHz, 0 °C (dynamic)): δ 8.13 (d, J = 8.4, 1H, An *p-H*), 8.10 (d, J = 8.4, 1H, An *p-H*′), 7.76 (br s, 8H, BAr′$_4$ *o-H*), 7.52 (br s, 4H, BAr′$_4$ *p-H*), 7.44−7.29 (m, 8H, An *m-H*, Ar *H*), 6.86 (d, J = 7.6, 1H, An *o-H*), 6.76 (d, J = 7.2, 1H, An *o-H*′), 2.31 and 2.24 (2 s, 6H each, Ar*Me*$_2$, Ar′*Me*$_2$), −0.14 (br s, 9H, Pd(C(C*H*$_3$)$_3$).

Trapping the agostic *tert*-butyl complex with acetonitrile yields the isobutyl acetonitrile complex, **[((2,6-(CH$_3$)$_2$C$_6$H$_3$)N═C(An)C(An)═N(2,6-(CH$_3$)$_2$C$_6$H$_3$))Pd(CH$_2$CH(CH$_3$)$_2$)(NCCH$_3$))]BAr′$_4$ (22a).** ^{1}H NMR (CD_2Cl_2, 400 MHz, −60 °C): δ 8.12 (d, J = 8.4, 1H, An *p-H*), 8.10 (d, J = 8.4, 1H, An *p-H*′), 7.72 (br s, 8H, BAr′$_4$ *o-H*), 7.53 (br s, 4H, BAr′$_4$ *p-H*), 7.47 (m, 2H, An *m-H*), 7.36−7.18 (m, 6H, Ar *H*), 6.96 (d, J = 7.2, 1H, An *o-H*), 6.50 (d, J = 7.2, 1H, An *o-H*′), 2.27 and 2.18 (2 s, 6H each, Ar*Me*$_2$, Ar′*Me*$_2$), 1.80 (s, 3H, Pd−NC*Me*), 1.48 (d, J = 7.2, 2H, Pd(C*H*$_2$CH(CH$_3$)$_2$)), 0.69 (d, J = 6.4, 6H, Pd(CH$_2$CH(C*H*$_3$)$_2$)), Pd(CH$_2$C*H*(CH$_3$)$_2$ obscured.

Trapping the agostic *tert*-butyl complex with ^{13}CO at −80 °C initially yields the *tert*-butyl carbonyl complex, **[((2,6-(CH$_3$)$_2$C$_6$H$_3$)N═C(An)C-(An)═N(2,6-(CH$_3$)$_2$C$_6$H$_3$))Pd(C(CH$_3$)$_3$)(*^{13}CO))]BAr′$_4$ (23a).** ^{1}H NMR ($CDCl_2F$, 400 MHz, −90 °C): δ 8.08 (d, J = 7.6, 1H, An *p-H*), 8.06 (d, J = 7.6, 1H, An *p-H*′), 7.77 (br s, 8H, BAr′$_4$ *o-H*), 7.52 (br s, 4H, BAr′$_4$ *p-H*), 7.50−7.21 (m, 8H, An *m-H*, Ar *H*), 6.78 (d, J = 7.6, 1H, An *o-H*), 6.23 (d, J = 7.6, 1H, An *o-H*′), 2.27 and 2.16 (2 s, 6H each, Ar*Me*$_2$, Ar′*Me*$_2$), 0.99 (s, 9H, Pd(C(C*H*$_3$)$_3$). ^{13}C NMR ($CDCl_2F$, 100 MHz, −90 °C): δ 180.9 (Pd(*^{13}CO), broadened due to exchange with free ^{13}CO).

The *tert*-butyl carbonyl complex isomerizes at −60 °C to give the isobutyl carbonyl complex, **[((2,6-(CH$_3$)$_2$C$_6$H$_3$)N═C(An)C(An)═N-(2,6-(CH$_3$)$_2$C$_6$H$_3$))Pd(CH$_2$CH(CH$_3$)$_2$)(*^{13}CO))]BAr′$_4$ (24a).** ^{1}H NMR ($CDCl_2F$, 400 MHz, −90 °C): δ 8.13−8.08 (m, 2H, An *p-H*, partially obscured by *tert*-butyl carbonyl complex), 7.77 (br s, 8H, BAr′$_4$ *o-H*), 7.52 (br s, 4H, BAr′$_4$ *p-H*), 7.52−7.22 (m, 8H, An *m-H*, Ar *H*), 6.83 (d, J = 7.2, 1H, An *o-H*), 6.49 (d, J = 7.2, 1H, An *o-H*′), 2.31 and 2.19 (2 s, 6H each, Ar*Me*$_2$, Ar′*Me*$_2$), 2.01 (d, J = 7.2, 2H, Pd(C*H*$_2$-CH(CH$_3$)$_2$)), 1.56 (m, 1H, Pd(CH$_2$C*H*(CH$_3$)$_2$)), 0.75 (d, J = 6.0, 6H, Pd(CH$_2$CH(C*H*$_3$)$_2$)). ^{13}C NMR ($CDCl_2F$, 100 MHz, −90 °C): δ 175.0 (sharp, Pd(*^{13}CO)).

The isobutyl carbonyl complex undergoes insertion between −60 and −40 °C to give the isobutyl acyl carbonyl complex, **[((2,6-(CH$_3$)$_2$C$_6$H$_3$)N═C(An)C(An)═N(2,6-(CH$_3$)$_2$C$_6$H$_3$))Pd(*^{13}C(O)CH$_2$CH-(CH$_3$)$_2$)(*^{13}CO))]BAr′$_4$ (25a).** ^{1}H NMR ($CDCl_2F$, 400 MHz, −40 °C): δ 8.12 (d, J = 8.4, 1H, An *p-H*), 8.09 (d, J = 8.4, 1H, An *p-H*′), 7.76 (br s, 8H, BAr′$_4$ *o-H*), 7.55−7.48 (m, 2H, An *m-H*), 7.53 (br s, 4H, BAr′$_4$ *p-H*), 7.36−7.25 (m, 6H, Ar *H*), 6.83 (d, J = 7.2, 1H, An *o-H*), 6.57 (d, J = 7.2, 1H, An *o-H*′), 2.64 (dd, $^2J_{CH}$ = 6.0, $^3J_{HH}$ = 6.0, 2H, Pd(*^{13}C(O)C*H*$_2$CH(CH$_3$)$_2$)), 2.32 and 2.31 (2 s, 6H each, Ar*Me*$_2$, Ar′*Me*$_2$), 0.56 (d, J = 6.4, 6H, Pd(*^{13}C(O)CH$_2$CH(C*H*$_3$)$_2$)), Pd(*^{13}C(O)CH$_2$C*H*(CH$_3$)$_2$) obscured. ^{13}C NMR ($CDCl_2F$, 100 MHz, −40 °C): δ 210.7 (sharp, Pd(*^{13}*C*(O)CH$_2$CH(CH$_3$)$_2$)), 172.2 (broad, Pd(*^{13}CO)).

[((2,6-(*i*-Pr)$_2$C$_6$H$_3$)N═C(An)C(An)═N(2,6-(*i*-Pr)$_2$C$_6$H$_3$))Pd(C(CH$_2$-μ-H)(CH$_3$)$_2$)]BAr′$_4$ (18b). ^{1}H NMR ($CDCl_2F$, 400 MHz, −130 °C (static)): δ 7.92 (d, J = 7.2, 1H, An *p-H*), 7.89 (d, J = 7.2, 1H, An *p-H*′), 7.71 (br s, 8H, BAr′$_4$ *o-H*), 7.44 (br s, 4H, BAr′$_4$ *p-H*), 7.46−

7.34 (m, 8H, An *m-H*, Ar *H*), 6.63 (d, $J = 7.2$, 1H, An *o-H*), 6.33 (d, $J = 7.2$, 1H, An *o-H′*), 2.97 (2 overlapping septets, 2H each, C*H*Me$_2$, C′*H*Me$_2$), 1.31, 1.23, 0.98, and 0.72 (4 br d, 6H each, CH*Me*Me′, CHMe*Me′*, C′H*Me*Me′, C′HMe*Me′*), 0.60 (br s, 6H, Pd(C(CH$_2$-μ-H)-(C*H*$_3$)$_2$)), −7.12 (br t, $J = 15$, 1H, Pd(C(CH$_2$-μ-*H*)(CH$_3$)$_2$), Pd(C(C*H*$_2$-μ-H)(CH$_3$)$_2$) obscured. ^{1}H NMR (CDCl$_2$F, 400 MHz, 0 °C (dynamic)): δ 8.04 (d, $J = 7.5$, 1H, An *p-H*), 8.01 (d, $J = 7.8$, 1H, An *p-H′*), 7.71 (br s, 8H, BAr′$_4$ *o-H*), 7.48 (br s, 4H, BAr′$_4$ *p-H*), 7.54−7.36 (m, 8H, An *m-H*, Ar *H*), 6.75 (d, $J = 7.2$, 1H, An *o-H*), 6.50 (d, $J = 7.2$, 1H, An *o-H′*), 3.11 and 3.10 (2 septets, 2H each, $J = 6.9$ and 6.6, C*H*Me$_2$, C′*H*Me$_2$), 1.36, 1.32, 1.05, and 0.82 (4d, 6H each, $J = 6.9$, 6.9, 6.6, 6.6, CH*Me*Me′, CHMe*Me′*, C′H*Me*Me′, C′HMe*Me′*), −0.20 (sharp s, 9H, Pd(C(C*H*$_3$)$_3$).

Trapping the agostic *tert*-butyl complex with acetonitrile yields the isobutyl acetonitrile complex, **[((2,6-(*i*-Pr)$_2$C$_6$H$_3$)N=C(An)C(An)=N-(2,6-(*i*-Pr)$_2$C$_6$H$_3$))Pd(CH$_2$CH(CH$_3$)$_2$)(NCCH$_3$)]BAr′$_4$ (22b).** ^{1}H NMR (CD$_2$Cl$_2$, 400 MHz, −60 °C): δ 8.13 (d, $J = 7.8$, 1H, An *p-H*), 8.11 (d, $J = 7.8$, 1H, An *p-H′*), 7.72 (br s, 8H, BAr′$_4$ *o-H*), 7.53 (br s, 4H, BAr′$_4$ *p-H*), 7.48−7.39 (m, 8H, An *m-H*, Ar *H*), 6.98 (d, $J = 6.9$, 1H, An *o-H*), 6.37 (d, $J = 7.5$, 1H, An *o-H′*), 3.20 and 3.12 (2 septets, 2H each, $J = 6.9$ and 6.0, C*H*Me$_2$, C′*H*Me$_2$), 1.77 (s, 3H, Pd−NC*Me*), 1.63 (d, 2H, $J = 7.2$, Pd(C*H*$_2$CH(CH$_3$)$_2$)), 1.38, 1.34, 1.00, and 0.84 (4d, 6H each, $J = 6.9$, 6.9, 6.6, 6.6, CH*Me*Me′, CHMe*Me′*, C′H*Me*Me′, C′HMe*Me′*), 0.76 (d, $J = 6.6$, 6H, Pd(CH$_2$CH(C*H*$_3$)$_2$)), Pd(CH$_2$C*H*(CH$_3$)$_2$ obscured.

Alkyl Ethylene Complexes. [((2,6-(CH$_3$)$_2$C$_6$H$_3$)N=C(An)C(An)=N(2,6-(CH$_3$)$_2$C$_6$H$_3$))Pd(CH$_2$CH$_3$)(CH$_2$=CH$_2$)]BAr′$_4$ (30a[BAr′$_4$]). ^{1}H NMR (CD$_2$Cl$_2$, 400 MHz, −80 °C): δ 8.17 .(d, $J = 8.0$, 1H, An *p-H*), 8.13 (d, $J = 8.0$, 1H, An *p-H′*), 7.71 (br s, 8H, BAr′$_4$ *o-H*), 7.53 (m, 2H, An *m-H*), 7.53 (br s, 4H, BAr′$_4$ *p-H*), 7.35 (m, 6H, Ar *H*), 6.71 (d, $J = 7.2$, 1H, An *o-H*), 6.64 (d, $J = 7.2$, 1H, An *o-H′*), 4.60 (br s, 4H, Pd(C*H*$_2$=C*H*$_2$)), 2.26 (s, 6H, ArC*H*$_3$), 2.21 (s, 6H, Ar′C*H*$_3$), 1.34 (q, $J = 7.2$, 2H, PdC*H*$_2$CH$_3$), 0.43 (t, $J = 7.2$, 3H, PdCH$_2$C*H*$_3$).

[((2,6-(CH$_3$)$_2$C$_6$H$_3$)N=C(An)C(An)=N(2,6-(CH$_3$)$_2$C$_6$H$_3$))Pd(CH$_2$-CH$_3$)(CH$_2$=CH$_2$)]HB(C$_6$F$_5$)$_3$ (30a[HB(C$_6$F$_5$)$_3$]). ^{1}H NMR (CD$_2$Cl$_2$, 500 MHz, −80 °C): δ 8.18 (d, $J = 8.3$, 1H, An *p-H*), 8.13 (d, $J = 8.3$, 1H, An *p-H′*), 7.52 (m, 2H, An *m-H*), 7.34 (m, 6H, Ar *H*), 6.66 (d, $J = 7.3$, 1H, An *o-H*), 6.59 (d, $J = 7.3$, 1H, An *o-H′*), 4.54 (s, 4H, Pd(C*H*$_2$=C*H*$_2$)), 3.4 (v br, 1H, *H*B(C$_6$F$_5$)$_3$), 2.24 (s, 6H, ArC*H*$_3$), 2.19 (s, 6H, Ar′C*H*$_3$), 1.23 (q, $J = 7.3$, 2H, PdC*H*$_2$CH$_3$), 0.38 (t, $J = 7.3$, 3H, PdCH$_2$C*H*$_3$).

[((2,6-(*i*-Pr)$_2$C$_6$H$_3$)N=C(An)C(An)=N(2,6-(*i*-Pr)$_2$C$_6$H$_3$))Pd(CH$_2$-CH$_3$)(CH$_2$=CH$_2$)]BAr′$_4$ (30b[BAr′$_4$]). ^{1}H NMR (CD$_2$Cl$_2$, 400 MHz, −80 °C): δ 8.07 (d, $J = 7.6$, 1H, An *p-H*), 8.03 .(d, $J = 8.0$, 1H, An *p-H′*), 7.71 (br s, 8H, BAr′$_4$ *o-H*), 7.55−7.38 (m, 8H, An *m-H*, Ar *H*), 7.53 (br s, 4H, BAr′$_4$ *p-H*), 6.50 (d, $J = 7.2$, 1H, An *o-H*), 6.44 (d, $J = 7.6$, 1H, An *o-H′*), 4.58 (br s, 4H, Pd(C*H*$_2$=C*H*$_2$), dynamic), 2.99 and 2.92 (2 septets, $J = 6.4$ and 6.4, 2H each, ArC*H*MeMe′, ArC′*H*MeMe′), 0.56 (q, $J = 7.2$, 2H, PdC*H*$_2$CH$_3$), 1.33, 1.28, 0.85, and 0.79 (4 d, $J = 6.4$, 6.4, 6.4, and 6.4, 6H each, CH*Me*Me′, CHMe*Me′*, C′H*Me*Me′, C′HMe*Me′*), 0.33 (t, $J = 7.2$, 3H, PdCH$_2$C*H*$_3$).

[((2,6-(*i*-Pr)$_2$C$_6$H$_3$)N=C(An)C(An)=N(2,6-(*i*-Pr)$_2$C$_6$H$_3$))Pd(CH$_2$-CH$_3$)(CH$_2$=CH$_2$)]HB(C$_6$F$_5$)$_3$ (30b[HB(C$_6$F$_5$)$_3$]). ^{1}H NMR (CD$_2$Cl$_2$, 400 MHz, −80 °C): δ 8.17 (d, $J = 8.0$, 1H, An *p-H*), 8.13 (d, $J = 8.0$, 1H, An *p-H′*), 7.48 (m, 8H, An *m-H*, Ar *H*), 6.53 (d, $J = 7.6$, 1H, An *o-H*), 6.45 (d, $J = 7.6$, 1H, An *o-H′*), 4.59 (s, 4H, Pd(C*H*$_2$=C*H*$_2$)), 3.4 (v br, 1H, *H*B(C$_6$F$_5$)$_3$), 3.00 and 2.93 (2 septets, $J = 6.8$ and 6.4, 2H each, ArC*H*MeMe′, ArC′*H*MeMe′), 1.57 (q, $J = 7.3$, 2H, PdC*H*$_2$-CH$_3$), 1.35, 1.29, 0.86, and 0.81 (4 d, $J = 6.8$, 6.8, 6.4, and 6.4, 6H each, CH*Me*Me′, CHMe*Me′*, C′H*Me*Me′, C′HMe*Me′*), 0.35 (t, $J = 7.3$, 3H, PdCH$_2$C*H*$_3$).

[((2,6-(CH$_3$)$_2$C$_6$H$_3$)N=C(An)C(An)=N(2,6-(CH$_3$)$_2$C$_6$H$_3$))Pd(CH-(CH$_3$)CH$_2$CH$_3$)(CH$_2$=CH$_2$)]BAr′$_4$ (36a). ^{1}H NMR (CD$_2$Cl$_2$, 400 MHz, −90 °C): δ 8.10 .(d, $J = 8.0$, 1H, An *p-H*), 8.06 .(d, $J = 8.4$, 1H, An *p-H′*), 7.77 (br s, 8H, BAr′$_4$ *o-H*), 7.53−7.45 (m, 2H, An *m-H*), 7.51 (br s, 4H, BAr′$_4$ *p-H*), 7.40−7.21 (m, 6H, Ar *H*), 6.63 (d, $J = 7.2$, 1H, An *o-H*), 6.60 (d, $J = 6.8$, 1H, An *o-H′*), 4.56 (m, 2H, Pd(C*H*H′=CH*H′*)), 4.53 (m, 2H, Pd(CH*H′*=C*H*H′)), 2.25, 2.21, and 2.18 (3 br s, 12H total, ArC*H*$_3$, ArC*H*$_3$′, Ar′C*H*$_3$, Ar′C*H*$_3$′), 1.67 (m, 1H, Pd-(C*H*(CH$_3$)CH$_2$CH$_3$)), 0.61 (m, 3H, Pd(CH(C*H*$_3$)CH$_2$CH$_3$)), 0.50 (m, 3H, Pd(CH(CH$_3$)CH$_2$C*H*$_3$)), Pd(CH(CH$_3$)C*H*$_2$CH$_3$) obscured.

[((2,6-(CH$_3$)$_2$C$_6$H$_3$)N=C(An)C(An)=N(2,6-(CH$_3$)$_2$C$_6$H$_3$))Pd(CH$_2$-CH$_2$CH$_2$CH$_3$)(CH$_2$=CH$_2$)]BAr′$_4$ (37a). ^{1}H NMR (CDCl$_2$F, 400 MHz, −50 °C): δ 8.13 (d, $J = 8.4$, 1H, An *p-H*), 8.09 (d, $J = 8.0$, 1H, An *p-H′*), 7.77 (br s, 8H, BAr′$_4$ *o-H*), 7.51 (br s, 4H, BAr′$_4$ *p-H*), 7.38 (m, 2H, An *m-H*), 7.35 (m, 6H, Ar *H*), 6.72 (d, $J = 7.2$, 1H, An *o-H*), 6.71 (d, $J = 7.2$, 1H, An *o-H′*), 4.60 (s, 4H, Pd(C*H*$_2$=C*H*$_2$)), 2.28 (s, 6H, ArC*H*$_3$), 2.22 (s, 6H, Ar′C*H*$_3$), 1.28, 1.01, and 0.72 (m, 2H each, PdC*H*$_2$C*H*$_2$CH$_2$CH$_3$), 0.56 (t, $J = 7.2$, 3H, PdCH$_2$CH$_2$CH$_2$C*H*$_3$).

[((2,6-(*i*-Pr)$_2$C$_6$H$_3$)N=C(An)C(An)=N(2,6-(*i*-Pr)$_2$C$_6$H$_3$))Pd(CH-(CH$_3$)CH$_2$CH$_3$)(CH$_2$=CH$_2$)]BAr′$_4$ (36b). ^{1}H NMR (CDCl$_2$F, 400 MHz, −90 °C): δ 8.01 (d, $J = 8.4$, 1H, An *p-H*), 7.97 (d, $J = 8.4$, 1H, An *p-H′*), 7.78 (br s, 8H, BAr′$_4$ *o-H*), 7.57 (br s, 4H, BAr′$_4$ *p-H*), 7.48 (m, 6H, An *m-H*, Ar *H*), 6.50 (d, $J = 7.2$, 1H, An *o-H*), 6.37 (d, $J = 7.2$, 1H, An *o-H′*), 4.68 (m, 2H, Pd(C*H*H′=CH*H′*)), 4.60 (m, 2H, Pd-(CH*H′*=C*H*H′)), 3.15 and 3.05 (2 septets, 2H each, ArC*H*MeMe′, ArC′*H*MeMe′), 2.05 (m, 1H, Pd(C*H*(CH$_3$)CH$_2$CH$_3$)), 1.40, 1.35, 0.90, and 0.80 (4 d, $J = 6.5$, 6.5, 6.8, and 6.8, 6H each, CH*Me*Me′, CHMe*Me′*, C′H*Me*Me′, C′HMe*Me′*), 0.70 (d, $J = 6.4$, 3H, Pd(CH-(C*H*$_3$)CH$_2$CH$_3$)), 0.36 (m, 3H, Pd(CH(CH$_3$)CH$_2$C*H*$_3$)), Pd(CH(CH$_3$)C*H*$_2$-CH$_3$) obscured.

[((2,6-(*i*-Pr)$_2$C$_6$H$_3$)N=C(An)C(An)=N(2,6-(*i*-Pr)$_2$C$_6$H$_3$))Pd(CH$_2$-CH$_2$CH$_2$CH$_3$(CH$_2$=CH$_2$)]BAr′$_4$ (37b). ^{1}H NMR (CDCl$_2$F, 400 MHz, −50 °C): δ 8.07 (d, $J = 8.0$, 1H, An *p-H*), 8.03 (d, $J = 8.0$, 1H, An *p-H′*), 7.77 (br s, 8H, BAr′$_4$ *o-H*), 7.54 (br s, 4H, BAr′$_4$ *p-H*), 7.5 (m, 6H, An *m-H*, Ar *H*), 6.59 (d, $J = 8.0$, 1H, An *o-H*), 6.55 (d, $J = 8.0$, 1H, An *o-H′*), 4.68 (s, 4H, Pd(C*H*$_2$=C*H*$_2$)), 3.08 and 3.00 (2 septets, $J = 6.8$ and 6.8, 2H each, ArC*H*MeMe′, ArC′*H*MeMe′), 1.56 (m, 2H, Pd(C*H*$_2$CH$_2$CH$_2$CH$_3$)), 1.42, 1.38 (2 d, $J = 6.8$, 6.8, 6H each, CH*Me*Me′, CHMe*Me′*), 0.97 (m, 2H, Pd(CH$_2$CH$_2$C*H*$_2$CH$_3$)), 0.92, 0.89 (2 d, $J = 6.8$, 6.8, 6H each, C′H*Me*Me′, C′HMe*Me′*), 0.58 (t, $J = 7.2$, 3H, Pd(CH$_2$CH$_2$CH$_2$C*H*$_3$)), Pd(CH$_2$C*H*$_2$CH$_2$CH$_3$) obscured.

[((2,6-(CH$_3$)$_2$C$_6$H$_3$)N=C(An)C(An)=N(2,6-(CH$_3$)$_2$C$_6$H$_3$))Pd(CH$_2$CH-(CH$_3$)$_2$)(CH$_2$=CH$_2$)]BAr′$_4$ (35a). ^{1}H NMR (CD$_2$Cl$_2$, 400 MHz, −80 °C): δ 8.14 (d, $J = 8.4$, 1H, An *p-H*), 8.10 .(d, $J = 8.4$, 1H, An *p-H′*), 7.72 (br s, 8H, BAr′$_4$ *o-H*), 7.51 (br s, 4H, BAr′$_4$ *p-H*), 7.49 (m, 2H, An *m-H*), 7.35−7.26 (m, 6H, Ar *H*), 6.67 (d, $J = 7.2$, 1H, An *o-H*), 6.62 (d, $J = 7.2$, 1H, An *o-H′*), 4.54 (s, 4H, Pd(C*H*$_2$=C*H*$_2$)), 2.19 and 2.16 (2 s, 6H each, Ar*Me*$_2$, Ar′*Me*$_2$), 1.20 (d, $J = 6.4$, 2H, Pd(C*H*$_2$-CH(CH$_3$)$_2$)), 0.62 (d, $J = 5.6$, 6H, Pd(CH$_2$CH(C*H*$_3$)$_2$)), Pd(CH$_2$C*H*(CH$_3$)$_2$) obscured.

[((2,6-(*i*-Pr)$_2$C$_6$H$_3$)N=C(An)C(An)=N(2,6-(*i*-Pr)$_2$C$_6$H$_3$))Pd(CH$_2$CH-(CH$_3$)$_2$)(CH$_2$=CH$_2$)]BAr′$_4$ (35b). ^{1}H NMR (CD$_2$Cl$_2$, 400 MHz, −80 °C): δ 8.06 (d, $J = 8.4$, 1H, An *p-H*), 8.02 (d, $J = 8.4$, 1H, An *p-H′*), 7.72 (br s, 8H, BAr′$_4$ *o-H*), 7.51 (br s, 4H, BAr′$_4$ *p-H*), 7.47 (m, 2H, An *m-H*), 7.40 (m, 6H, Ar *H*), 6.52 (d, $J = 7.6$, 1H, An *o-H*), 6.44 (d, $J = 7.2$, 1H, An *o-H′*), 4.58 (s, 4H, Pd(C*H*$_2$=C*H*$_2$)), 2.98 and 2.94 (2 septets, $J = 6.4$ and 6.4, 2H each, ArC*H*MeMe′, ArC′*H*MeMe′), 1.38 (d, $J = 6.8$, 2H, Pd(C*H*$_2$CH(CH$_3$)$_2$)), 1.33, 1.28 (2 d, $J = 6.4$, 6.4, 6H each, CH*Me*Me′, CHMe*Me′*), 0.95 (m, 1H, Pd(CH$_2$C*H*(CH$_3$)$_2$)), 0.80 (m, 12H, C′H*Me*Me′, C′HMe*Me′*), 0.61 (d, $J = 5.6$, 6H, Pd(CH$_2$CH-(C*H*$_3$)$_2$)).

Rates of Migratory Insertion, Dissociation, and Association: NMR Spectroscopy. (a) Ethyl Ethylene Migratory Insertion. Rates for migratory insertion of ethylene into the Pd−ethyl bond were determined by adding 20 equiv of ethylene to the ethyl ethylene complexes (BAr′$_4$ counterion; spectra are described above) and monitoring the loss of the Pd(CH$_2$C*H*$_3$)$_2$ resonance (ca. 0.4 ppm) over time (BAr′$_4$ *p*-H was used as an internal standard). The natural logarithm of the methyl integral was plotted versus time (first-order treatment) to obtain kinetic plots (see Supporting Information). Three kinetic runs were done for each species, and the averages are reported in Table 3.

(b) Isobutyl Ethylene Migratory Insertion. A similar method was used for determining the rate of migratory insertion for the isobutyl ethylene complex **35b**. Loss of the isobutyl methyl resonance was monitored with respect to time, and the average barriers obtained are also reported in Table 3.

(c) Ethylene Dissociation. Rates for ethylene dissociation from the ethyl ethylene complex **30b**[HB(C$_6$F$_5$)$_3$] were determined by monitoring the loss of the labeled CH$_2$ resonance in the ^{1}H NMR spectrum with time. These data was treated as a first-order reaction approaching equilibrium (see Supporting Information for plot).

(d) Associative Exchange of Ethylene. The rate of exchange of bound ethylene with free ethylene in complexes **30a,b**[$HB(C_6F_5)_3$] was determined by NMR line broadening experiments at −85 °C in CD_2Cl_2. Samples were prepared by the reaction of the diethyl complexes **31a,b** with a stoichiometric amount of $B(C_6F_5)_3$, generating the ethyl ethylene complexes **30a,b**[$HB(C_6F_5)_3$] in situ. After the ^1H NMR spectrum was acquired in the absence of exchange, ethylene was added to the NMR tube via gastight syringe and a second spectrum was obtained at the same temperature. The amount of ethylene in solution was calculated using the acenaphthyl *ortho* hydrogens as an internal standard. Line widths (ω) were measured at half-height in units of Hz for complexed ethylene and were corrected for line widths (ω_o) in the absence of exchange. Second-order associative exchange rates were determined from the standard equation for the slow exchange approximation, $k = \pi(\omega - \omega_o)/[C_2H_4]$, where $[C_2H_4]$ is the molar concentration of free ethylene. A pulse delay of 60 s was used. (The T_1 of free ethylene is 15 s.) These experiments were repeated twice, and the average second-order rate constants are reported in Table 2.

Migratory Insertion Rate Ratios: Gas Chromatography. Ratios of rate constants were obtained by GC for primary versus secondary insertion using the butyl ethylene complexes (**36a**/**37a** and **36b**/**37b**) and propyl ethylene complexes (**9b**/**10b**) described above. A representative procedure is outlined here for complexes **36b**/**37b**. A small, flame-dried Schlenk flask was charged with **28b** (38.3 mg, 0.025 mmol) in an argon-filled drybox. The flask was cooled to −78 °C, and CH_2Cl_2 (2.5 mL) was added via syringe. Ethylene (0.61 mL, 0.025 mmol) was added to the orange solution via gastight syringe. The flask was rapidly warmed to −20 °C and was stirred at this temperature for 10 min. The reaction was then quenched by the addition of excess $HSiEt_3$ (0.1 mL). The volatile products were then vacuum transferred away from the Pd material and analyzed by GC. The following temperature program was employed: injector temperature, 250 °C; detector temperature, 250 °C; initial temperature, 35 °C; initial time, 15 min; ramp rate, 20 °C/min; final temperature, 250 °C; final time, 15 min. Peaks were identified by elution time on the basis of standards run separately as solutions in CH_2Cl_2. Retention times were as follows: 5.63 min (ethylene); 5.95 min (*n*-propane); 6.43 min (2-methyl propane); 6.77 min (*n*-butane); 8.00 min (2-methyl butane); 8.86 (*n*-pentane); 9.04 min (diethyl ether); 9.55 min (methylene chloride); 10.14 min (2,2-dimethylbutane); 11.92 min (2-methylpentane); 12.89 min (3-methylpentane); 14.30 min (*n*-hexane); 20.21 min (*n*-heptane); 22.07 min (triethylsilane); 24.09 min (*n*-octane).

Acknowledgment. The authors wish to thank the NSF (Grant CHE-0107810) and DuPont for funding. L.H.S. acknowledges the NSF for a graduate research fellowship. M.B. thanks the Humboldt Foundation for support during preparation of the manuscript.

Supporting Information Available: Preparation and spectral details for **13b**, **14a,b**, and **15a,b** and graphs for the determination of rates of migratory insertion for **30a,b**[BAr'_4] and **35a,b** and ethylene dissociation in **30b**[$HB(C_6F_5)_3$]. This material is available free of charge via the Internet at http://pubs.acs.org.

JA011055J